Synthesis of Potent Cytotoxic Epidithiodiketopiperazines Designed for Derivatization

Chase R. Olsson[†], **Joshua N. Payette**[†], **Jaime H. Cheah**[‡], **Mohammad Movassaghi**[*,†]

[†]Department of Chemistry, Massachusetts Institute of Technology, Cambridge, Massachusetts 02139, USA

[‡]The Koch Institute for Integrative Cancer Research, Massachusetts Institute of Technology, 500 Main Street, Cambridge, Massachusetts 02139, United States

Abstract

We describe our design, synthesis, and chemical study of a set of functional epidithiodiketopiperazines (ETPs) and evaluation of their activity against five human cancer cell lines. Our structure-activity relationship-guided substitution of ETP alkaloids offers versatile derivatization, while maintaining potent anticancer activity, offering exciting opportunity for their use as there are no examples of complex and potently anticancer (nM) ETPs being directly used as conjugatable probes or warheads. Our synthetic solutions to strategically designed ETPs with functional linkers required advances in stereoselective late-stage oxidation and thiolation chemistry in complex settings, including the application of novel reagents for dihydroxylation and *cis*-sulfidation of diketopiperazines. We demonstrate that complex ETPs equipped with a strategically substituted azide functional group are readily derivatized to the corresponding ETP-triazoles without compromising anticancer activity. Our chemical stability studies of ETPs along with cytotoxic evaluation of our designed ETPs against A549, DU 145, HeLa, HCT 116, and MCF7 human cancer cell lines provide insights into the impact of structural features on potency and chemical stability, informing future utility of ETPs in chemical and biological studies.

Graphical Abstract

---
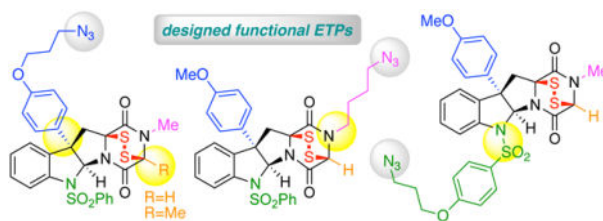
[*]**Corresponding Author**: movassag@mit.edu.

Introduction

Epipolythiodiketopiperazine alkaloids comprise a structurally diverse and biologically active family of fungal metabolites characterized by a polysulfide bridged 2,5-diketopiperazine substructure (Figure 1).[1,2,3,4] These natural products possess myriad biological activities including anticancer,[4,5] antifungal,[6] antibacterial,[6,7] and antiviral properties,[8] and thus have prompted considerable interest in chemistry and allied sciences.[9 , 10] While the mechanism of action of these compounds is not precisely understood, the pivotal role of the polysulfide bridge for bioactivity is well appreciated.[1,4–8] At least three pathways of toxicity have been proposed in the literature[1,4–8] for ETP-containing compounds: (1) redox cycling generating deleterious reactive oxygen species (ROS) (*e.g.*, superoxide radical anion, hydroxyl radical, hydrogen peroxide) and causing oxidative stress, DNA strand cleavage, and apoptosis;[5b] (2) disruption of the global tertiary structures of proteins and/or inhibition of protein function due to thiol-disulfide exchange;[5a,e] and (3) disruption of zinc-binding proteins by promoting intramolecular protein disulfide formation concomitant with zinc ion (or zinc ETP complex) ejection.[5c,6,8] Our previous structure-activity relationship (SAR) study of a diverse set of cyclotryptophan-containing epipolythiodiketopiperazines for cytotoxic activity against several human cancer cell lines[4] inspired our pursuit of synthetic epidithiodiketopiperazines (ETPs) with strategic substitution that enhances their translational potential as chemical probes[11] and anticancer payloads.[12] Herein, we describe our design and synthesis of complex ETPs (Figure 2), their chemical study and derivatization, along with their cytotoxicity against A549, DU 145, HeLa, HCT 116, and MCF7 human cancer cell lines.

Our SAR study[4] identified the dimeric ETP (+)–**4** (Figure 1), a bis-sulfonyl derivative[9a] of the natural product (+)–dideoxyverticillin A (**1**),[13] as a highly potent anticancer compound against five human cancer cell lines. Additionally, we recognized minimal required structural features in complex cyclotryptophan-ETPs for optimal cytotoxicity as well as strategic positions of the common substructure that allow substitution with minimal impact on anticancer activity.[4] For example, the activity of N1-benzenesulfonyl substituted derivative (+)–**4** was increased by up to two orders of magnitude compared to the natural product (+)–dideoxyverticillin A (**1**) {(+)–**4** *vs.* (+)–**1**; IC_{50} (U-937, histiocytic lymphoma): 0.18 nM *vs.* 15.5 nM; IC_{50} (HeLa, cervical carcinoma): 0.09 nM *vs.* 7.2 nM; IC_{50} (NClH460, lung carcinoma): 1.53 nM *vs.* 42 nM; IC_{50} (786-O, renal carcinoma): 1.55 nM *vs.* 33.5 nM; IC_{50} (MCF7, breast carcinoma): 1.65 nM *vs.* 28.4 nM}.[14] Likewise, the unnatural C3-aryl ETP (+)–**8**, a truncated analog of dimeric alkaloid (+)–**1**, maintained ample cytotoxicity against the same panel of cell lines {IC_{50} (U-937): 5.0 nM; IC50 (HeLa): 26.8 nM; IC_{50} (NCl-H460): 46.7 nM; IC_{50} (786-O): 83 nM; IC_{50} (MCF7): 63 nM}. The readily accessible ETP (+)–**8** offers an opportunity for the design and the development of functional ETPs for use in detailed chemical and biological investigations.

Results and Discussion

Design and Synthesis of Complex ETP-Azides (+)–9a–c.

We targeted compounds (+)–**9a**–**c** (Figure 2) guided by the insights gained in our prior SAR study.[4] We envisioned C3, N1, and N14 (for positional numbering system, see Figure S1) as optimal positions for introduction of a functional handle for further chemical modification

while maintaining the cytotoxicity of ETP (+)–**8**. Herein, we report the synthesis of functional ETPs (+)–**9a**–**c**. Lacking full C15-substitution, these ETPs avoid the often seen challenges concerning C15-epimerization or elimination of alanine- or serine-derived diketopiperazine (DKP) precursors.[2,9] The synthesis of ETPs (+)–**9a** and (+)–**9b** from sarcosine streamlined their preparation,[15] whereas ETP (+)–**9c** required the development of a DKP N-alkylation strategy. Additionally, informed by mechanistic studies on the potent yet chemically sensitive C15-H substituted ETPs (vide infra), we designed C15-Me substituted ETP (+)–**9d** as a variant of ETP (+)–**9a** with improved chemical stability. Our syntheses of ETPs (+)–**9a**–**d** and related derivatives leverage advances in late-stage oxidation and thiolation strategies, including the application of a novel thiolating reagent for stereoselective introduction of two C–S bonds onto a DKP. Additionally, we provide a platform for rapid derivatization and conjugation of complex ETPs. The presence of the alkyl azide and the compatibility of the sensitive epidisulfide-bridge with the planned copper(I)-catalyzed azide-alkyne cycloaddition (CuAAC) reaction[16] enabled the facile conjugation of these designed ETPs as potent anticancer payloads (vide infra). Bioactive small molecules have been structurally modified[17] and used in various contexts including antibody-drug conjugates for targeted drug delivery,[12] activity-based protein profiling,[18] photoaffinity labels for target identification,[19] small molecule imaging probes,[20] and polymer-drug conjugates for improved pharmacokinetics.[21] While advances in synthesis of ETPs continue to enable informative biochemical studies,[22] there are no examples of complex and potently anticancer (nM) ETPs being directly used as conjugatable probes or warheads as described here. We anticipate that the functional alkyl azide handle on our designed ETPs provides a versatile strategy for ligation of complex ETPs using CuAAC, providing exciting new opportunities for chemical and biological studies.

We designed ETP (+)–**9a** (Scheme 1) with an alkyl azide incorporated via C3-substitution based on our observations that aryl substituents at C3 of the cyclotryptophan substructure of ETPs led to an increase in potency relative to short chain alkyl substituents.[4] Our synthesis of ETP (+)–**9a** commenced with treatment of *endo*-tetracyclic bromide (+)–**10**[4] with aryl ether **11**[23] under our silver-promoted C3-arylation of cyclotryptophan-DKPs[24] to provide the desired Friedel-Crafts product in 78% yield. Epimerization of the base-sensitive C11 stereocenter during desilylation was completely suppressed by employing hydrogen fluoride in a mixture of pyridine and THF to furnish alcohol (+)–**12** in 90% yield as a single diastereomer.[25] Conversion of alcohol (+)–**12** into the corresponding azide (+)–**13**, via the Bose-Mitsunobu protocol with polymer-supported triphenylphosphine (PPh$_3$•PS),[26] set the stage for the planned stereoselective DKP dihydroxylation[2,27] and sulfidation.[2–4,9] Exposure of azide (+)–**13** to tetra*n*-butylammonium permanganate[28] in 1,2-dichloroethane gave diol (−)-**14** in 63% yield as a single diastereomer.[2] Introduction of the critical epidisulfide bridge was achieved by treatment of diol (−)–**14** with trifluoroacetic acid in a saturated solution of hydrogen sulfide in nitroethane, followed by oxidative disulfide formation upon exposure to potassium triiodide[9a] to afford C3-functionalized ETP-azide (+)–**9a** in 65% yield.

As illustrated in Scheme 2, the synthesis of N1-substituted ETP-azide (+)–**9b** necessitated early introduction of the azide functional group via N1-sulfonylation. The condensation of the readily prepared carboxylic acid (−)–**15**[23] with sarcosine methyl ester hydrogen chloride,

promoted by *N*-[(dimethylamino)-1*H*-1,2,3-triazolo-[4,5-*b*]pyridin1-ylmethylene]-*N*-methylmethanaminium hexafluorophosphate *N*-oxide (HATU) afforded the corresponding dipeptide in 73% yield. Subsequent deprotection of the *tert*-butoxycarbonyl group with trifluoroacetic acid in dichloromethane followed by treatment with morpholine in *tert*-butanol resulted in cyclization to DKP (−)−**16** in 99% yield.[9a,29] Exposure of DKP (−)−**16** to bromine[29] in dichloromethane afforded *endo*-tetracyclic bromide (+)−**17** in 79% yield and >18:1 dr. Application of our methodologies2 for C3-arylation (99%),[24] permanganate-promoted DKP dihydroxylation (46%),[27] and sulfidation[4,9] of diol (−)−**19** provided N1-functionalized ETP-azide (+)−**9b** in 64% yield.

Considering the presence of N14-substitution in the vast majority of ETP natural products,[1,5–8] we designed ETP (+)−**9c** (Scheme 3) consistent with parameters described above to incorporate the alkyl azide via N14-substitution. Our synthesis of ETP-azide (+)−**9c** began with N-alkylation of diketopiperazine (+)−**20**.[23] However, direct N-alkylation of (+)−**20** with alkyl iodide or allyl bromide derivatives resulted in no reactivity or low conversions, respectively, with significant C11 epimerization. We hypothesized that converting the electron withdrawing C3bromide to the desired aryl substitution may enhance nucleophilicity of N14 and suppress C11 epimerization. Furthermore, we postulated the use of a propargylic electrophile might provide superior N-alkylation. Under optimal conditions, treatment of C3-aryl diketopiperazine (+)−**21** with lithium hexamethyldisilylamide (LHMDS) in a mixture of *N,N'*-dimethylpropyleneurea–tetrahydrofuran (DMPU–THF, 1:4) at −30 °C followed by addition of propargyl bromide **22** afforded alkyne (+)−**23** in 60% yield.[23] Hydrogenation of benzyl ether (+)−**23** proved challenging due to competitive reduction of a putative allylic alcohol/ether intermediate that gave rise to an undesired N14-*n*-butyl derivative of alcohol (+)−**24**.[30] Temporal control of the reduction events was achieved by means of a solvent change, wherein alkyne (+)−**23** was subjected to palladium on carbon (Pd/C, 5 wt.%) in ethyl acetate under an atmosphere of dihydrogen to fully reduce the alkyne functional group, followed by dilution of the reaction mixture with ethanol to hydrogenolyze the benzyl protective group and to afford alcohol (+)−**24** in 93% yield. The remaining steps to ETP-azide (+)−**9c** follow our general synthetic strategy described in the synthesis of ETP-azide (+)−**9a**, involving the application of the Bose-Mitsunobu[26] azidation chemistry to afford DKP-azide (+)−**25** in 67% yield, permanganate-mediated hydroxylation27 to give DKP-diol (+)−**26** in 48% yield, nucleophilic DKPsulfidation,[4,9] and subsequent triiodide-promoted disulfide formation9a to give N14-functionalized ETP-azide (+)**9c** in 50% yield.

Synthesis of Derivatized ETP-Triazoles (+)−28a–c.

With ETP-azides (+)−**9a**–**c** in hand we next evaluated the compatibility of the sensitive epidisulfide-based warhead with the planned CuAAC reaction.[16] We employed 4-ethynylanisole (**27**) as a model substrate for CuAAC-based conjugation of complex ETPs with alkyne tethered partners (Table 1). Importantly, treatment of a solution of ETP-azides (+)−**9a**–**c** with alkyne **27** and copper iodide31 at 23 °C proceeded smoothly to provide the corresponding triazoles (+)−**28a**–**c** in 94%, 57%, and 85%32 yield, respectively. We next obtained promising IC$_{50}$ values (vida infra) for both ETP-azides and the corresponding triazoles, as discussed below in greater detail (Table 2), and determined that conjugated

ETP-triazoles (+)–**28a**–**c** retain the potent anticancer activity of their ETP-azide precursors. This observation highlights the outstanding potential for use of complex and potently anticancer ETP-azides as ready-to-conjugate payloads for synthesis of probes and future use in targeted delivery.[11,12,17–21]

Derivatization of Functional Linker.

The ability to couple our ETP azides with bifunctional alkynes also provides an expedient opportunity for final stage diversification of the functional linker. For example, where introduction of a primary amine may be of interest for ligation and further derivatization,[33] such as bioconjugation[11,12,18–20] or synthesis of a focused library using acyl donors,[34] the conjugation of *N*-Bocpropargylamine with ETP-azide (+)–**9a** directly affords the protected ETP-amine (+)–**29** in 89% yield (Scheme 4). Unraveling of the primary amine under acidic conditions followed by direct acylation with benzoyl chloride, as a model acyl donor,[34] affords ETP-amide (+)–**30** in 87% yield, highlighting the versatility of our ETP-azide derivatives for rapid diversification.

Chemical Stability Studies and Design Enhancement Based on C15-Substitution.

We next aimed to better understand the chemical stability of our synthetic ETPs to inform their future use. To this end, we chose to study the stability of ETP (+)–**8** (Scheme 5) under conditions relevant to common conjugation reactions. Importantly, ETP (+)–**8** can be recovered intact and with excellent mass balance from critical control experiments involving exposure to bioconjugation conditions[35] such as those used in amidation of an activated ester[36] or incubation in cellular lysing buffer (pH 7.4) for 24 h.[37] However, the observed formation of minor side products in our studies, including sulfur-congeners of ETP (+)–**8**, prompted a deeper investigation. To facilitate these mechanistic studies, we independently prepared possible decomposition products including the corresponding epitrisulfide **31** (Scheme 5) and epitetrasulfide **32** to confirm their detection.[23] While ETP (+)–**8** is stable in deuterochloroform [20 mM] at 23 °C over 20 h as monitored by 1H NMR analysis, introduction of triethylamine (2 equiv) led to gradual consumption of ETP (+)–**8** (~15%) and concomitant formation of epitrisulfide **31** (~5%) over 20 h. Similar observations were made using Hünig's base and DABCO as the base additive, and the rate of decomposition was greater using higher dielectric constant media including acetonitrile, dimethylsulfoxide, and *N,N*-dimethylformamide. For example, treatment of ETP (+)–**8** with triethylamine (2 equiv) in DMF [20 mM] for 2 h (Scheme 5) led to isolation of epitrisulfide **31** (8%) and epitetrasulfide **32** (11%), as well as diketopiperazinethione **34a** (3%) and corresponding hydrolysis product, triketopiperazine **34b** (3%), diketopiperazinethione **35a** (16%) and triketopiperazine **35b** (5%).[38] As highlighted in Scheme 5, our hypothesis for formation of these side products, under the basic conditions described above, involves H15 deprotonation of ETP (+)–**8** resulting in S-S bond scission and formation of intermediate thiol **33**, a reactive species that leads to consumption of the starting disulfide and ultimately give rise to the higher order polysulfanes via electrophilic sulfur transfer.[2,9b] A plausible mechanism for the degradation of ETP (+)–**8** and formation of its congeners **31**–**32** is depicted in Scheme S1.[23]

We hypothesized the C15-Me substitution of alanine-derived ETP (+)−**42** (Scheme 6) could avoid the decomposition pathway described above and provide a more stable ETP. While our earlier SAR studies suggested that alanine based ETPs were approximately an order of magnitude less active than their sarcosine analogues,[4] we envisioned the additional C15-substitution would translate to enhanced stability and a superior mechanistic probe. Due to the expected altered reactivity profile of C15-substitution,[2–4,9] the synthesis of epidisulfide (+)−**42** also offered opportunities to refine our hydroxylation and sulfidation strategies en route to ETPs. As illustrated in Scheme 6, silver-mediated activation[24] of bromide (+)−**36**[2,24] gave C3–adduct (+)−**37** in 81% yield. We found that permanganate-mediated dihydroxylation using bis(2,2'-bipyridyl)-copper(II) permanganate {bipy$_2$Cu(MnO$_4$)$_2$}[39] proved particularly effective in furnishing DKP-diol **38** as a single diastereomer in 74% yield.[40] This represents the first application of this mild oxidant for DKP dihydroxylation. The impact of the counter-ion on the outcome of the permanganate-promoted oxidation of diketopiperazines is consistent with our prior observations and mechanistic studies.[2,27] The tactical conversion of diol **38** to an alcohol by monosilylation (84%) resulted in a mixture of regioisomeric (1.1:1) monosilylether alcohols with improved stability and solubility characteristics,[9a] setting the stage for stereoselective introduction of the epidisulfide bridge.

As part of an ongoing effort to advance the selectivity and efficiency of our methodology in accessing ETPs,[2] we discovered a practical reagent that can be used to give *cis*-sulfidation en route to epidisulfide (+)−**42** and its sulfurcongeners. After establishing that independent exposure of either monosilyl regioisomer derivative of diol **38** (Scheme 6) to potassium trithiocarbonate[9a] and trifluoroacetic acid in dichloromethane led to formation of dithiepanethione (+)−**41** in moderate yield (66–73%), we hypothesized if a suitably designed alkyl trithiocarbonate derivative could enhance the overall efficiency through superior reagent solubility and stability. As illustrated in Scheme 6, we found that monosodium trithiocarbonate **39**, conveniently prepared from commercially available *p*-methoxybenzyl thiol,[23] without the use of dihydrogen sulfide, gave dithiepanethione (+)−**41** in 85% yield, likely via efficient formation of sulfonium ion **40**. The versatile dithiepanethione (+)−**41** was efficiently converted to the ETP (+)−**42** in 87% yield upon aminolysis to a bisthiol intermediate followed by oxidative disulfide formation. Additionally, exposure of the same bisthiol intermediate to sulfur dichloride and disulfur dichloride provided the epitrisulfide **43** (Scheme 6) and epitetrasulfide **44** in 22% and 66% yield, respectively.[23]

Synthesis of Bisdisulfides via Thiol-Disulfide Exchange.

In comparison to C15-desmethyl ETP (+)−**8**, the enhanced chemical stability of C15-substituted ETP (+)−**42** provided an excellent opportunity to investigate the reactivity of the epidisulfide-bridge in thiol-disulfide exchange reactions. Consistent with the stability studies described above (Scheme 5), exposure of a solution of C15-desmethyl ETP (+)−**8** in deuteroacetonitrile [20 mM] to triethylamine (2.2 equiv) at 23 °C led to complete consumption of epidisulfide (+)−**8** over 2 h as observed by in situ 1H NMR monitoring experiments, followed by the isolation of epitrisulfide **31** (16%) and epitetrasulfide **32** (24%). Conversely, exposure of C15-substituted ETP (+)−**42** to identical conditions led to no decomposition and allowed quantitative recovery of ETP (+)−**42**. Given the importance of ETP's reactivity with cellular thiols for its biological activity,[1,5–8,41,42] we set out to study

disulfide exchange reactions using ETPs (+)–**8**, (+)–**42**, and the corresponding mixed bisdisulfides. Our SAR profile of ETPs demonstrated bisdisulfides also served as competent anticancer agents.[4] We hypothesized that these species might serve as prodrugs, being converted to their corresponding epidisulfide pharmacophores under biological conditions, which are then concentrated within the cell via thiolmediated uptake.[42]

As illustrated in Scheme 7, treatment of ETP (+)–**42** with excess (*para*-fluorobenzyl)disulfane (10 equiv) in the presence of *para*-fluorobenzylthiol (1.0 equiv) and triethylamine (2.5 equiv) in THF [0.1 M] at 23 °C for 65 h resulted in isolation of bis(*para*-fluorobenzyl)disulfide **45a** in 22% yield, alongside the recovery of ETP (+)–**42** in 66% yield.[23] This exchange reaction could be monitored with 1H NMR experiments by diluting aliquots of the reaction mixture into deuterochloroform; we found that the 3:1 equilibrium ratio favoring ETP (+)–**42**, consistent with isolated yields, could be established from either direction by treating either (+)–**42** or **45a** under identical conditions (see Scheme S2).[23] In parallel studies, we found that C15-desmethyl ETP (+)–**8** could be converted to the corresponding bisdisulfide **45b** (Scheme 7), but that analogous disulfide-exchange equilibration experiments resulted in the appearance of undesired sulfur-congeners trisulfide **31** and tetrasulfide **32** (Scheme 5). Specifically, treatment of epidisulfide (+)–**8** with excess (*para*-fluorobenzyl)disulfane (3.0 equiv) in the presence of *para*fluorobenzylthiol (0.5 equiv) and triethylamine (2.0 equiv) in THF [20 mM] at 23 °C for 30 min afforded bisdisulfide **45b** (69%), epitrisulfide **31** (2%), and recovered epidisulfide (+)–**8** (17%).[43] Notably, exposure of bisdisulfide **45b** to identical conditions resulted in a mixture of di-, tri-, and tetra-sulfides consistent with our earlier observations (Scheme 5).

We next aimed to evaluate the feasability of bisdisulfides undergoing reversion to epidisulfides under biologically relevant, aqueous conditions. We prepared water-soluble glutathione bisdisulfide **46** (Scheme 7) in 45% isolated yield by stepwise reduction with sodium borohydride and subsequent exposure of the crude bisthiol to electrophilic S-(phenylsulfonyl)-L-glutathione[44] (5 equiv) and triethylamine (11 equiv) in a mixture of methanol and tetrahydrofuran.[23] Monitoring by ^{1}H NMR spectroscopy, we found that exposure of bisdisulfide **46** to L-glutathione (1.0 equiv) and triethylamine (1.0 equiv) in deuterium oxide–deuteroacetonitrile [2:3, 2 mM] led to formation of epidisulfide (+)–**42** in 15 minutes (Scheme 7, **42**:**46**, >50:1).[45] As mixed bisdisulfides **45a**, **45b**, and **46** readily revert to their respective ETP derivative, our thiol-disulfide exchange studies highlight the remarkable thermodynamic stability of the ETP substructure but also present a potential strategy to modulate ETP cytotoxicity in prodrug form.

Design and Synthesis of Complex ETP-Azide (+)–9d.

Having demonstrated the superior stability of alanine-derived ETPs, we chose to prepare C15-Me substituted functional ETP (+)–**9d** (Scheme 8). We were guided by comparisons in the activities (vida infra) of ETPs (+)–**9a–c** to prepare C3-functionalized ETP (+)–**9d**, keeping the N1 and N14 substitutions for added stability and potency as described above. The synthesis of ETP (+)–**9d** parallels our strategy described above for synthesis of related ETPs, beginning with C3-arylation[24] of bromide (+)–**36**[9a] with aryl silyl ether **11** (73%). Removal of the silyl ether to give alcohol (+)–**47** (96%) followed by conversion to the

corresponding azide (85%)[23] afforded the DKP (+)−**48**. Application of our DKP sulfidation strategy involved oxidation of DKP (+)−**48** to give diol **49** in 65% yield, which upon exposure to *t*-butyldimethylsilyl chloride gave a regioisomeric mixture of monosilyl monoalcohols (1.1:1) in 85% yield. Consistent with our observation in synthesis of ETP (+) −**42** and use of monosilyl ether intermediates, exposure of the regioisomeric monosilyl ethers to nitroethane saturated with hydrogen sulfide gas followed by oxidation with triiodide gave the desired C15-substituted C3-functionalized ETP azide (+)−**9d** in 53% yield. Efforts to apply potassium trithiocarbonate or monosodium trithiocarbonate **39** towards the *cis*-sulfidation of diol **49** or its corresponding monosilyl ether intermediates were unsuccessful due to the competitive reduction of the alkyl azide. To further highlight the diversity of linkers that we may couple with our functional ETPs without compromising anticancer activity, we conjugated epidisulfide probe (+)−**9d** with ethylene glycol-derived alkyne **50** through application of the CuAAC coupling strategy, affording triazole **51** in 92% yield. The protected amine in ETP **51** can be derivatized as demonstrated in Scheme 4. We anticipate the superior stability of ETP (+)−**9d** may result in clearer biochemical readouts when used in mechanistic studies.

Anticancer Activity of Designed ETP Derivatives.

The evaluation of our model and functionalized ETP probes as anticancer agents against a panel of five human cancer cell lines is illustrated in Table 2. A range of complex derivatives including ETPs (+)−**4**, (+)−**8**, and (+)−**42**, ETP-azides (+)−**9a–d**, and ETP-triazole conjugates (+)**28a–c**, (+)−**29**, and **51**, in addition to bisdisulfides **45a**, **45b**, and **46** were evaluated for cytotoxicity against cervical carcinoma (HeLa), alveolar adenocarcinoma (A549), breast adenocarcinoma (MCF7), colorectal carcinoma (HCT 116), and prostate carcinoma (DU 145) cell lines. Importantly, our designed ETPs displayed similar patterns of potency in the form of low nanomolar cytotoxicity across all cell lines examined in this study.

Comparisons between ETPs (+)−**8** and (+)−**42**, along with their respective functionalized ETP-azide derivatives (+)−**9a–c** and (+)−**9d**, indicate that ETPs possessing conjugatable chemical handles about either the C3, N1, or N14 positions are well tolerated (Table 2). While we demonstrated that C15-substituted ETP (+)−**42** is chemically more stable than glycine-derived ETP (+)−**8** (Scheme 5), glycine-derived ETPs were more active against the same cell lines {(+)−**42** *vs.* (+)−**8**: IC_{50} (HeLa): 32 *vs.* 5.5 nM; IC_{50} (A549): 92 *vs.* 16 nM; IC_{50} (MCF7): 81 *vs.* 9.2 nM; IC_{50} (HCT 116): 374 *vs.* 6.9 nM; IC_{50} (DU 145): 36 *vs.* 3.4 nM}. The degree to which the sarcosine-derived ETPs (+)−**9a–c** maintained cytotoxicity compared to dimeric ETP (+)−**4**, despite only having a single epidisulfide bridge, may in part be due to greater access to the epidisulfane bridge lacking substitution at C15. In comparing model ETP (+)−**8** to its functionalized derivatives ETP-azides (+)−**9a–c**, we found the activity of ETP (+)−**9a** to be unaffected across all five cell lines (<2-fold difference), (+)−**9b** to be slightly reduced {(+)−**9b** *vs.* (+)−**8**: IC_{50} (HeLa): 3-fold decrease; IC_{50} (A549): 5-fold decrease; IC_{50} (MCF7): 6-fold decrease; IC_{50} (HCT 116): 5-fold decrease; IC_{50} (DU 145): 13-fold decrease}, and (+)−**9c** to be most impaired {(+)−**9c** *vs.* (+) −**8**: IC_{50} (HeLa): 8-fold decrease; IC_{50} (A549): 9-fold decrease; IC_{50} (MCF7): 6-fold decrease; IC_{50} (HCT 116): 15-fold decrease; IC_{50} (DU 145): 19-fold decrease}. Similarly,

functionalization of C15-Me substituted ETP (+)−**42** as ETP-azide (+)−**9d** did not impact the activity against MCF7 or HCT 116 cell lines, but resulted in slightly reduced activities against HeLa, A549, and DU 145 cell lines {(+)−**9d** *vs.* (+)−**42**: IC_{50} (HeLa): 136 *vs.* 32 nM; IC_{50} (A549): 251 *vs.* 92 nM; IC_{50} (DU 145): 306 *vs.* 36 nM}.

As illustrated in Table 2, triazole conjugates of ETP-azides (+)−**9a**–**d** prepared using CuAAC chemistry largely retain the anticancer potency. The conversion of azide (+)−**9a** to triazole (+)−**28a** resulted in a minimal (<3-fold) loss of activity across all five cell lines, whereas an analogous comparison between azide (+)−**9b** and triazole (+)**28b** resulted in a minimal (2- to 3-fold) increase in activity upon conjugation. Compared to azide (+)−**9c**, triazole (+)−**28c** was slightly more active (4-fold) against MCF7 and HCT 116 cell lines and (2- to 3-fold) against HeLa, A549, and DU 145 cell lines. Interestingly, the derivatization of ETP-azide (+)−**9d** as PEG-triazole **51** increased the activity for HeLa and DU 145 cell lines (5-fold), resulting in activities comparable to parent ETP (+)−**42** {**51** *vs.* (+)−**42**; IC_{50} (HeLa): 24 *vs.* 32 nM; IC_{50} (A549): 116 *vs.* 92 nM; IC_{50} (MCF7): 82 *vs.* 81 nM; IC_{50} (HCT 116): 148 *vs.* 374 nM; IC_{50} (DU 145): 62 *vs.* 36 nM} as well as the C15-desmethyl triazole (+)−**29**. The anticancer potency of both our ETP-azides and their corresponding conjugated ETP-triazoles highlights the exciting opportunity for their use as biochemical probes and in targeted delivery.

Expanding on our prior observations[4] that bisdisulfides derived from ETPs retain anticancer activity, we found that the composition of the mixed disulfide impacts anticancer activity (Table 2). For example, whereas bis(*para*-fluorobenzyl)-disulfides **45a** and **45b** have similar activities to their parent ETPs (+)−**42** and (+)−**8**, respectively, the larger bis(L-glutathione)disulfide **46** derived from ETP (+)−**42** was significantly less active {**46** *vs.* (+)−**42**; IC_{50} (HeLa): 508 *vs.* 32 nM; IC_{50} (A549): 910 *vs.* 92 nM; IC_{50} (MCF7): 500 *vs.* 81 nM; IC_{50} (HCT 116): 1096 *vs.* 374 nM; IC_{50} (DU 145): 580 *vs.* 36 nM}. The reduced activity of bis(L-glutathione)disulfide **46** compared to bis(*para*-fluorobenzyl)disulfides **45a** and **45b** is likely due to a combination of factors including cellular permeability, pharmacodynamic properties, steric crowding at the sulfur atoms, and variation in the reduction potentials.[46] The application of these bisdisulfides as ETP prodrugs may find utility in the treatment of cancers with higher glutathione (GSH) to glutathione disulfide (GSSG) ratios. For example, several studies have found that invasive and metastatic colon and prostate tumors have higher extracellular thiol concentrations than healthy tissue.[47] Our observations suggest possible modulation of ETP toxicity in pro-drug form as the corresponding bisdisulfides for a more controlled ETP formation at the local tumor environment with higher GSH concentration.

Conclusions

In summary, we have described the design, synthesis, chemical stability studies, and evaluation of functional ETPs as potent anticancer compounds. Our SAR informed strategic substitution of designed ETPs (+)−**9a**–**c** with an alkyl azide at the C3, N1, and N14 positions, respectively, enabled versatile derivatization while maintaining potency. Employing sarcosine as starting material streamlined the synthesis of ETP-azides (+)−**9a** and (+)−**9b**, whereas ETP-azide (+)−**9c** required the development of a mild diketopiperazine

N-alkylation strategy. Mechanistic studies and cytotoxic evaluation of the potent C15-H substituted ETPs (+)–**8** and (+)–**9a–c** led us to design C15-Me substituted ETP-azide (+)–**9d** to reduce the rate of base-promoted decomposition of the ETP warhead. Our synthetic solutions to these complex ETPs required advances in stereoselective late-stage dihydroxylation and sulfidation strategies, including the application of novel reagents for dihydroxylation and *cis*-sulfidation of diketopiperazines. While C15-H substituted ETP-azides (+)–**9a–c** offer outstanding anticancer activity, the C15-Me substituted ETP-azide (+)–**9d** with its enhanced chemical stability may provide more clear readouts when used in biochemical studies. The results of our thiol-disulfide exchange studies revealed that mixed bisdisulfides **45a**, **45b**, and **46** readily revert to their respective ETPs, *demonstrating the remarkable thermodynamic stability of the ETP substructure as well as revealing a potential strategy to modulate ETP cytotoxicity and pharmacodynamics in pro-drug form.* The facile conjugation of ETP-azides (+)–**9a–d** using CuAAC chemistry provides a flexible approach for further functionalization of complex ETPs, affording access to corresponding ETP-triazoles without compromising anticancer activity. Our findings highlight the outstanding potential for diversification of functional ETP-azides to enhance their translational potential as chemical probes or anticancer warheads.

EXPERIMENTAL SECTION

General Methods.

All reactions were performed in oven-dried or flame-dried round-bottom flasks, modified Schlenk (Kjeldahl shape) flasks, or glass pressure vessels. The flasks were fitted with rubber septa, and reactions were conducted under a positive pressure of argon. Cannulae or gas-tight syringes with stainless steel needles were used to transfer air- or moisture-sensitive liquids. Flash column chromatography was performed as described by Still[48] using granular silica gel (60-Å pore size, 40–63 μm, 4–6% H_2O content) or C_{18}-reversed-phase silica gel (90-Å pore size, 40–63 μm). Analytical thin layer chromatography (TLC) was performed using glass plates pre-coated with 0.25 mm 230–400 mesh silica gel impregnated with a fluorescent indicator (254 nm) or basic alumina impregnated with a fluorescent indicator (254 nm). Thin layer chromatography plates were visualized by exposure to short wave ultraviolet light (254 nm) and/or irreversibly stained by treatment with an aqueous solution of ceric ammonium molybdate (CAM), an ethanolic solution of phosphomolybdic acid (PMA), an aqueous solution of silver nitrate ($AgNO_3$), Ellman's reagent (5,5'-dithiobis-(2-nitrobenzoic acid), DTNB) in *N*,*N*-dimethylformamide,[49] or an aqueous solution of potassium permanganate ($KMnO_4$), followed by heating (~ 1 min) on a hot plate (~250 °C). Organic solutions were concentrated at 30 °C on rotary evaporators capable of achieving a minimum pressure of ~2 Torr. Proton (^1H) and carbon (^{13}C) nuclear magnetic resonance spectra were recorded with 600 MHz, 500 MHz, or 400 MHz spectrometers. Proton nuclear magnetic resonance (^1H NMR) spectra are reported in parts per million on the δ scale and are referenced from the residual protium in the NMR solvent ($CHCl_3$: δ 7.26, CD_2HCN: 1.94, CD_2HOD: 3.31, CD_3SOCD_2H: 2.50, H_2O: 4.79).[50] Data are reported as follows: chemical shift [multiplicity (s = singlet, d = doublet, t = triplet, q = quartet, p = pentet, m = multiplet, br = broad), coupling constant(s) in Hertz, integration, assignment]. Broadband proton-decoupled carbon-13 nuclear magnetic resonance ($^{13}C\{^1H\}$ NMR) spectra are

reported in parts per million on the δ scale, and are referenced from the carbon resonances of the solvent (CDCl$_3$: δ 77.16, CD$_3$CN: 118.26, CD$_3$OD: 49.00, DMSO-d_6: 39.52). Structural assignments were made with additional information from gCOSY, gHSQC, and gHMBC experiments. Infrared data (IR) were obtained with a FTIR or an ATR and are reported as follows: [frequency of absorption (cm^{-1}), intensity of absorption (s = strong, m = medium, w = weak, br = broad)]. Optical Rotations were recorded on a polarimeter and specific rotations are reported as follows: [wavelength of light, temperature (°C), specific rotation, concentration in grams/100 mL of solution, solvent]. Highresolution mass spectra (HRMS) were recorded on a FT-ICR-MS using electrospray (ESI) (*m/z*) ionization source or direct analysis in real time (DART), a Q-TOF LC/MS using ESI, or an AccuTOF LC/MS using DART.

Representative Procedure for C3-Derivatization: Synthesis of (+)–(5a*S*,10b*S*,11a*S*)-2-Methyl-6(phenylsulfonyl)-10b-(4-(3-((triisopropylsilyl)oxy)propoxy)phenyl-2,3,6,10b,11,11a-hexahydro-4*H*pyrazino[1',2':1,5]pyrrolo[2,3-*b*]indole-1,4(5a*H*)-dione (S2);[51] C3-adduct (+)–S2.

endo-Tetracyclic bromide (+)–**10** (1.67 g, 3.50 mmol, 1 equiv), 2,6-di-*tert*-butyl-4-methylpyridine (DTBMP, 1.81 g, 8.80 mmol, 2.51 equiv), and triisopropyl(3-phenoxypropoxy)silane (**11**, 2.16 g, 6.99 mmol, 2.00 equiv) were azeotropically dried by concentration from anhydrous benzene (30 mL) under reduced pressure. Dichloromethane (35 mL) was added via syringe, and silver hexafluoroantimonate (2.40 g, 6.99 mmol, 2.00 equiv) was added as a solid in one portion to the solution at 23 °C. After 1 h, the reaction mixture was diluted with dichloromethane (100 mL) and was filtered through a pad of diatomaceous earth. The filter cake was washed with dichloromethane (3 × 50 mL), and the filtrate was concentrated under reduced pressure. The resulting residue was purified by flash column chromatography on silica gel (eluent: 0→20% acetone in dichloromethane) to afford C3-adduct (+)–**S2** (1.93 g, 78%) as a white solid. ^{1}H NMR (400 MHz, CDCl$_3$, 25 °C): δ 7.58 (d, *J* = 8.1 Hz, 1H), 7.46 (app-d, *J* = 8.5 Hz, 2H, SO$_2$Ph), 7.30 (app-t, *J* = 7.5 Hz, 1H), 7.28–7.24 (m, 1H), 7.10 (m, 4H), 6.68–6.61 (m, 4H), 6.13 (s, 1H), 4.39 (app-t, *J* = 8.3 Hz, 1H), 4.10 (d, *J* = 17.4 Hz, 1H), 4.04 (t, *J* = 6.3 Hz, 2H), 3.86 (t, *J* = 6.1 Hz, 2H), 3.82 (d, *J* = 17.4 Hz, 1H), 3.06 (dd, *J* = 7.0, 14.1 Hz, 1H), 2.89–2.83 (m, 4H), 1.98 (p, *J* = 6.1 Hz, 2H), 1.11–1.03 (m, 21H). ^{13}C{^{1}H} NMR (100 MHz, CDCl$_3$, 25 °C): d 167.1, 165.2, 158.4, 139.9, 138.2, 135.8, 133.0, 132.5, 129.2, 128.7, 128.1, 128.0, 126.0, 125.4, 117.2, 115.0, 87.2, 64.9, 59.8, 59.4, 58.6, 54.5, 39.1, 33.7, 32.7, 18.2, 12.1. FTIR (thin film) cm^{-1}: 3065 (m), 2943 (s), 2868 (s), 1684 (s), 1610 (m), 1512 (m), 1253 (m), 1171 (m), 883 (m), 686 (w). HRMS (DART) *m/z*: [M + H]$^+$ calc'd for C$_{38}$H$_{50}$N$_3$O$_6$SSi 704.3184; Found 704.3195. [α]$_D$23: +19 (*c* = 0.24, CHCl$_3$). TLC (30% acetone in dichloromethane), R*f*: 0.63 (UV, CAM).

Representative Synthesis of a Base-Sensitive Azide Precursor: Synthesis of (+)–(5a*S*,10b*S*,11a*S*)-10b-(4-(3-Hydroxypropoxy)phenyl)-2-methyl-6-(phenylsulfonyl)-2,3,6,10b,11,11a-hexahydro-4*H*pyrazino[1',2':1,5]pyrrolo[2,3-*b*]indole-1,4(5a*H*)-dione (12);[51] alcohol (+)–12.

A freshly prepared solution of hydrogen fluoride–pyridine (70% HF, 9 mL), pyridine (18 mL), and tetrahydrofuran (72 mL) at 0 °C was poured into a solution of C3-adduct (+)–**S2**

(1.89 g, 2.69 mmol, 1 equiv) in tetrahydrofuran (90 mL) at 0 °C contained in a 1–L polypropylene vessel. After 5 min, the ice-water bath was removed and the solution was allowed to stir and warm to 23 °C. After 20 h, the reaction mixture was cooled to 0 °C and was diluted with a saturated aqueous sodium bicarbonate solution (500 mL) in portions (50 mL) over 15 min. The resulting mixture was extracted with ethyl acetate (300 mL), the layers were separated, and the aqueous layer was extracted with ethyl acetate (2×75 mL). The combined organic extracts were washed sequentially with a saturated aqueous copper(II) sulfate solution (3×100 mL), with a saturated aqueous ammonium chloride solution (3×100 mL), and with a saturated aqueous sodium chloride solution (75 mL). The organic layer was dried over anhydrous sodium sulfate, was filtered, and was concentrated under reduced pressure. The resulting residue was purified by flash column chromatography on silica gel (eluent: $0\rightarrow60\%$ acetone in dichloromethane) to afford alcohol (+)–**12** (1.33 g, 90%) as a white solid. 1H NMR (400 MHz, CDCl$_3$, 25 °C): δ 7.57 (d, $J = 8.1$ Hz, 1H), 7.45 (app-d, $J = 9.7$ Hz, 2H), 7.33 (app-t, $J = 7.5$ Hz, 1H), 7.28–7.23 (m, 1H), 7.12–7.08 (m, 4H), 6.65 (app-d, $J = 9.0$ Hz, 2H) 6.60 (app-d, $J = 9.0$ Hz, 2H), 6.13 (s, 1H), 4.41 (app-t, $J = 8.3$ Hz, 1H), 4.10 (d, $J = 17.3$ Hz, 1H), 4.05 (t, $J = 6.0$ Hz, 2H), 3.84 (t, $J = 6.0$ Hz, 2H), 3.81 (d, $J = 17.7$ Hz, 1H), 3.06 (dd, $J = 7.0, 14.1$ Hz, 1H), 2.88–2.82 (m, 4H), 2.02 (p, $J = 5.9$ Hz, 2H), 1.88 (br-s, 1H). ^{13}C{^{1}H} NMR (100 MHz, CDCl$_3$, 25 °C): δ 167.1, 165.3, 158.1, 139.9, 138.2, 135.9, 133.1, 132.9, 129.3, 128.8, 128.2, 127.6, 126.0, 125.5, 117.2, 115.0, 87.2, 65.8, 60.2, 59.4, 58.6, 54.4, 39.0, 33.7, 32.1. FTIR (thin film) cm^{-1}: 2954 (w), 1700 (s), 1684 (s), 1507 (m), 1362 (m), 1169 (m), 832 (w), 668 (m). HRMS (DART) m/z: [M + H]$^+$ calc'd for C$_{29}$H$_{30}$N$_3$O$_6$S 548.1850; Found 548.1872. [α]$_D$23: +26 ($c = 0.12$, CHCl$_3$). TLC (30% acetone in dichloromethane), Rf: 0.21 (UV, CAM).

Representative Azide Synthesis: Synthesis of (+)–(5a*S*,10b*S*,11a*S*)-10b-(4-(3-Azidopropoxy)phenyl)-2methyl-6-(phenylsulfonyl)-2,3,6,10b,11,11a-hexahydro-4*H*-pyrazino[1',2':1,5]pyrrolo[2,3-*b*]indole-1,4(5a*H*)-dione (13);[51] azide (+)–13.

Diisopropyl azodicarboxylate (DIAD, 256 μL, 1.28 mmol, 1.50 equiv) and diphenylphosphoryl azide (DPPA, 276 μL, 1.28 mmol, 1.50 equiv) were added dropwise via syringe to a suspension of alcohol (+)–**12** (466 mg, 851 μmol, 1 equiv) and resin–bound triphenylphosphine (1.31 mmol/g on 100–200 mesh polystyrene cross–linked with 1% divinylbenzene, 973 mg, 1.28 mmol, 1.50 equiv) in tetrahydrofuran (20 mL) at 0 °C. After 5 min, the ice-water bath was removed and the reaction mixture was allowed to stir and warm to 23 °C. After 16 h, the reaction mixture was filtered through a 1 cm pad of diatomaceous earth in a 60-mL medium-porosity fritted-glass funnel. The filter cake was washed with dichloromethane (100 mL), and the filtrate was concentrated under reduced pressure. The resulting residue was purified by flash column chromatography on silica gel (eluent: 30% acetone in dichloromethane) to afford azide (+)–**13** (425 mg, 87%) as a white solid. ^{1}H NMR (400 MHz, CDCl$_3$, 25 °C): δ 7.58 (d, $J = 8.1$ Hz, 1H), 7.49 (app-d, $J = 8.4$ Hz, 2H), 7.34 (app-t, $J = 7.5$ Hz, 1H), 7.28–7.23 (m, 1H), 7.14–7.09 (m, 4H), 6.68 (app-d, $J = 9.0$ Hz, 2H) 6.62 (app-d, $J = 9.0$ Hz, 2H), 6.13 (s, 1H), 4.39 (app-t, $J = 8.2$ Hz, 1H), 4.10 (d, $J = 17.4$ Hz, 1H), 3.99 (t, $J = 5.9$ Hz, 2H), 3.82 (d, $J = 17.4$ Hz, 1H), 3.51 (t, $J = 6.5$ Hz, 2H), 3.06 (dd, $J = 7.1, 14.2$ Hz, 1H), 2.89–2.83 (m, 4H), 2.04 (p, $J = 6.2$ Hz, 2H). ^{13}C{^{1}H} NMR (100 MHz, CDCl$_3$, 25 °C): δ 167.1, 165.3, 157.9, 139.9, 138.2, 135.8, 133.1, 133.0, 129.3, 128.7, 128.2, 127.7, 126.0, 125.4, 117.2, 115.0, 87.1, 64.7, 59.4, 58.6, 54.4, 48.3, 39.0, 33.7, 28.9.

FTIR (thin film) cm^{-1}: 2929 (w), 2099 (s), 1700 (s), 1684 (s), 1512 (m), 1362 (m), 1252 (m), 1169 (m), 1091 (w), 832 (w), 668 (m). HRMS (DART) m/z: [M + H]$^+$ calc'd for C$_{29}$H$_{29}$N$_6$O$_5$S 573.1915; Found 573.1921. [α]$_D$23: +21.8 (c = 0.22, CHCl$_3$). TLC (30% acetone in dichloromethane), Rf: 0.55 (UV, CAM).

Representative DKP-Dihydroxylation: Synthesis of (–)-(3*R*,5a*S*,10b*S*,11a*R*)-10b-(4-(3-Azidopropoxy) phenyl)-3,11a-dihydroxy-2-methyl-6-(phenylsulfonyl)-2,3,6,10b,11,11a-hexahydro-4*H*-pyrazino[1',2':1,5] pyrrolo[2,3-*b*]indole-1,4(5a*H*)-dione (14);[51] diol (–)-14.

Tetra-*n*-butylammonium permanganate[28] (807 mg, 2.23 mmol, 5.05 equiv) was added as a solid to a solution of azide (+)–**13** (253 mg, 442 μmol, 1 equiv) in 1,2-dichloroethane (16 mL) at 23 °C. After 1 h, the reaction mixture was diluted with a saturated aqueous sodium sulfite solution (50 mL) and with ethyl acetate-hexanes (9:1, 200 mL). The resulting mixture was washed with a saturated aqueous sodium bicarbonate solution (50 mL), the layers were separated, and the organic layer was washed sequentially with a saturated aqueous sodium bicarbonate solution (50 mL), with deionized water (50 mL), and with a saturated aqueous sodium chloride solution (25 mL). The combined aqueous layers were extracted with ethyl acetate-hexanes (9:1, 2 × 50 mL), and the combined organic extracts were dried over anhydrous sodium sulfate, were filtered, and were concentrated under reduced pressure. The resulting residue was purified by flash column chromatography on silica gel (eluent: 0→40% acetone in dichloromethane) to afford diol (–)–**14** (169 mg, 63%) as a white solid. ^{1}H NMR (400 MHz, DMSO-d$_6$, 25 °C): δ 7.43 (app-t, J = 7.4 Hz, 1H), 7.39–7.32 (m, 4H), 7.26–7.19 (m, 3H), 7.13 (app-t, J = 7.5 Hz, 2H), 7.01 (d, J = 7.2 Hz, 1H), 6.75 (app-d, J = 8.9 Hz), 6.66 (app-d, J = 8.9 Hz, 2H), 6.21 (s, 1H), 5.00 (d, J = 6.8 Hz, 1H), 4.02 (t, J = 6.0 Hz, 2H), 3.54 (t, J = 6.7 Hz, 2H), 3.19 (d, J = 14.9 Hz, 1H), 2.77 (s, 3H), 2.66 (d, J = 14.9 Hz, 1H), 1.99 (p, J = 6.3 Hz, 2H). ^{13}C{^{1}H} NMR (100 MHz, DMSO-d$_6$, 25 °C): δ 166.6, 165.8, 157.1, 139.3, 138.0, 137.7, 133.6, 133.2, 128.9, 128.7, 128.0, 126.7, 126.6, 125.7, 117.0, 114.5, 87.3, 86.0, 80.9, 64.6, 57.4, 49.7, 47.7, 30.5, 28.1. FTIR (thin film) cm–1: 2095 (m), 1844 (m), 1734 (m), 1700 (s), 1685 (s), 1653 (s), 1559 (s), 1540 (m), 1507 (m), 1457 (m), 1055 (w), 668 (m). HRMS (DART) m/z: [M + H]$^+$ calc'd for C$_{29}$H$_{29}$N$_6$O$_7$S 605.1813; Found 605.1814. [α]$_D$23: –6 (c = 0.16, DMSO). TLC (30% acetone in dichloromethane), Rf: 0.40 (UV, CAM).

Representative DKP-Sulfidation: Synthesis of (+)–(3*S*,5a*S*,10b*S*,11a*S*)-10b-(4-(3-Azidopropoxy)phenyl)2-methyl-6-(phenylsulfonyl)-2,3,5a,6,10b,11-hexahydro-3,11a-epidithiopyrazino[1',2':1,5]pyrrolo[2,3*b*]indole-1,4-dione;[51] epidithiodiketopiperazine azide (+)–9a.

A solution of diol (–)-**14** (190 mg, 314 μmol, 1 equiv) in anhydrous nitroethane (13 mL) at 0 °C was sparged with hydrogen sulfide gas for 20 min by discharge of a balloon equipped with a needle extending into the reaction mixture, providing a saturated hydrogen sulfide solution. Trifluoroacetic acid (TFA, 9.8 mL) was added via syringe over 20 seconds, and the sparging with hydrogen sulfide gas was maintained for another 20 min. The ice-water bath was removed and the solution was allowed to stir and warm to 23 °C under an atmosphere of hydrogen sulfide. After 2 h, the reaction mixture was diluted with ethyl acetate (125 mL), was slowly poured into a stirring saturated aqueous sodium bicarbonate solution (50 mL), and the organic layer was washed with a saturated aqueous sodium chloride solution (35

mL). A stock solution of potassium triiodide in pyridine[9a] was added dropwise into the organic layer containing crude bisthiol until a persistent yellow color was observed. The resulting mixture was washed with an aqueous hydrogen chloride solution (1 M, 2×35 mL), was washed with a saturated aqueous sodium chloride solution (35 mL), was dried over anhydrous sodium sulfate, was filtered, and was concentrated under reduced pressure. The resulting residue was purified by flash column chromatography on silica gel (eluent: $10{\rightarrow}20\%$ ethyl acetate in dichloromethane) to afford epidithiodiketopiperazine azide (+)−**9a** (129 mg, 65%) as a beige solid. ^{1}H NMR (400 MHz, CDCl$_3$, 25 °C): δ 7.59 (d, $J = 8.0$ Hz, 1H), 7.40–7.34 (m, 3H), 7.29 (app-t, $J = 7.5$ Hz, 1H), 7.25–7.21 (m, 2H), 7.03 (t, $J = 7.9$ Hz, 2H), 6.75 (app-d, $J = 8.9$ Hz, 2H), 6.61 (app-d, $J = 8.9$ Hz, 2H), 6.38 (s, 1H), 5.24 (s, 1H), 3.99 (t, $J = 6.0$ Hz, 2H), 3.62 (d, $J = 15.5$ Hz, 1H), 3.51 (t, $J = 6.5$ Hz, 2H), 3.11 (s, 3H), 2.84 (d, $J = 15.5$ Hz, 1H), 2.03 (p, $J = 6.1$ Hz, 2H). ^{13}C{^{1}H} NMR (100 MHz, CDCl$_3$, 25 °C): δ 165.2, 160.2, 158.1, 141.3, 138.5, 135.9, 133.1, 131.6, 129.9, 128.7, 128.1, 127.3, 126.2, 125.7, 119.0, 115.1, 87.7, 74.6, 68.5, 64.7, 59.6, 48.3, 45.5, 32.2, 28.9. FTIR (thin film) cm^{-1}: 2926 (w), 2098 (m), 1717 (s), 1700 (s), 1685 (s), 1559 (m), 1507 (m), 1473 (w), 972 (w), 668 (m). HRMS (DART) m/z: [M + NH$_4$]$^+$ calc'd for C$_{29}$H$_{30}$N$_7$O$_5$S$_3$ 652.1465; Found 652.1454. [α]$_D$23: +236 ($c = 0.10$, CHCl$_3$). TLC (20% ethyl acetate in dichloromethane), Rf: 0.32 (UV, CAM, AgNO$_3$).

Representative Procedure of CuAAC Ligation: Synthesis of (+) −(3S,5aS,10bS,11aS)-10b-(4-(3-(4-(4Methoxyphenyl)-1H-1,2,3-triazol-1-yl)propoxy)phenyl)-2-methyl-6-(phenylsulfonyl)-2,3,5a,6,10b,11hexahydro-3,11a-epidithiopyrazino[1',2':1,5]pyrrolo[2,3-b]indole-1,4-dione (28a);[51] triazole (+)−28a.

Copper (I) iodide (45.7 mg, 0.240 mmol, 1.50 equiv) was added as a solid to a solution of epidithiodiketopiperazine azide (+)−**9a** (102 mg, 0.160 mmol, 1 equiv), 4-ethynylanisole **27** (104 μL, 0.800 mmol, 5.00 equiv), acetic acid (28 μL, 0.48 mmol, 3.0 equiv), and N,N-diisopropylethylamine (84 μL, 0.48 mmol, 3.0 equiv) in dichloromethane (1.6 mL) at 23 °C. After 11 h, the reaction mixture was directly purified by flash column chromatography on silica gel (eluent: 20% ethyl acetate in dichloromethane→100% ethyl acetate) to afford triazole (+)−**28a** (116 mg, 94%) as a yellow solid. 1H NMR (400 MHz, CDCl$_3$, 25 °C): δ 7.70 (app-d, $J = 8.8$ Hz, 2H), 7.68 (s, 1H), 7.57 (d, $J = 8.0$ Hz, 1H), 7.39–7.35 (m, 3H), 7.30–7.19 (m, 3H), 7.03 (t, $J = 7.9$ Hz, 2H), 6.92 (app-d, $J = 8.8$ Hz, 2H), 6.76 (app-d, $J = 8.8$ Hz, 2H), 6.60 (app-d, $J = 8.8$ Hz, 2H), 6.38 (s, 1H), 5.21 (s, 1H), 4.61 (t, $J = 6.7$ Hz, 2H), 3.94–3.91 (m, 2H), 3.81 (s, 3H,), 3.62 (d, $J = 15.5$ Hz, 1H), 3.10 (s, 3H), 2.83 (d, $J = 15.5$ Hz, 1H), 2.42 (p, $J = 6.3$ Hz, 2H). 13C{1H} NMR (100 MHz, CDCl$_3$, 25 °C): δ 165.1, 160.1, 159.7, 157.8, 147.8, 141.3, 138.3, 135.8, 133.1, 131.7, 129.8, 128.6, 128.0, 127.2, 127.1, 126.2, 125.6, 123.3, 119.3, 118.9, 115.0, 114.4, 87.6, 74.5, 68.4, 64.3, 59.5, 55.4, 47.1, 45.4, 32.1, 30.0. FTIR (thin film) cm^{-1}: 3058 (m), 2958 (w), 1700 (s), 1646 (s), 1559 (m), 1512 (s), 1458 (m), 1250 (w), 1171 (s), 1032 (w), 836 (m). HRMS (ESI) m/z: [M + H]$^+$ calc'd for C$_{38}$H$_{35}$N$_6$O$_6$S$_3$ 767.1775; Found 767.1796. [α]$_D$23: +315 ($c = 0.10$, CHCl$_3$). TLC (100% ethyl acetate), Rf: 0.38 (UV, CAM, AgNO$_3$).

Representative Synthesis of ETP-Amine Acylation: Synthesis of (+) −N-((1-(3-(4-((3S,5aS,10bS,11aS)-2Methyl-1,4-dioxo-6-(phenylsulfonyl)-1,2,3,4,5a,6-

hexahydro-3,11a-epidithiopyrazino[1',2':1,5]pyrrolo[2,3*b*]indol-10b(11*H*)-yl)phenoxy)propyl)-1*H*-1,2,3-triazol-4-yl)methyl)benzamide (30);[51] benzamide (+)–30.

A solution of hydrogen chloride in 1,4-dioxane (4.0 M, 1.0 mL) was added via syringe to a solution of triazole (+)–**29** (15.0 mg, 19.0 μmol, 1 equiv) in 1,4-dioxane (0.5 mL) at 23 °C. After 20 min, the reaction mixture was concentrated under reduced pressure, and the resulting yellow solid was dissolved in pyridine (240 μL). A solution of benzoyl chloride (48 mM, 0.60 mL, 29 μmol, 1.5 equiv) in tetrahydrofuran was added via syringe, followed by the addition of triethylamine (40 μL, 290 μmol, 15 equiv) via syringe. After 30 min, the reaction mixture was diluted with ethyl acetate (30 mL) and was slowly poured into an aqueous hydrogen chloride solution (1 M, 5 mL). The organic layer was washed sequentially with an aqueous hydrogen chloride solution (1 M, 5 mL), with a saturated aqueous sodium bicarbonate solution (5 mL), and with a saturated aqueous sodium chloride solution (5 mL). The organic layer was dried over anhydrous sodium sulfate, was filtered, and was concentrated under reduced pressure. The resulting residue was purified by flash column chromatography on silica gel (eluent: 1→2% methanol in dichloromethane) to afford benzamide (+)–**30** (13.1 mg, 87%) as a beige solid. 1H NMR (400 MHz, CDCl$_3$, 25 °C): δ 7.77 (app-d, J = 7.3 Hz, 2H), 7.71 (br-s, 1H), 7.57 (d, J = 8.0 Hz, 1H), 7.46 (app-t, J = 7.4 Hz, 1H), 7.40–7.32 (m, 5H), 7.28–7.20 (m, 3H), 7.16 (br-s, 1H), 7.01 (app-t, J = 7.8 Hz, 2H), 6.71 (app-d, J = 8.8 Hz, 2H), 6.56 (app-d, J = 8.8 Hz, 2H), 6.36 (s, 1H), 5.27 (s, 1H), 4.68 (br-s, 2H), 4.55 (t, J = 6.3 Hz, 2H), 3.95–3.84 (m, 2H), 3.60 (d, J = 15.5 Hz, 1H), 3.10 (s, 3H), 2.83 (d, J = 15.5 Hz, 1H), 2.37 (p, J = 5.9 Hz, 2H). 13C{1H} NMR (150 MHz, CDCl$_3$, 25 °C): δ 167.6, 165.2, 160.2, 157.8, 145.0, 141.3, 138.4, 135.9, 134.0, 133.2, 131.9, 131.8, 129.9, 128.8, 128.7, 128.1, 127.3, 127.2, 126.3, 125.7, 123.3, 119.0, 115.1, 87.7, 74.6, 68.5, 64.3, 59.5, 47.4, 45.5, 35.5, 32.2, 30.0. FTIR (thin film) cm^{-1}: 3345 (w), 3001 (w), 1695 (s), 1512 (m), 1461 (m), 1169 (m), 755 (m). HRMS (ESI) m/z: [M + H]$^+$ calc'd for C$_{39}$H$_{36}$N$_7$O$_6$S$_3$ 794.1884; Found 794.1890. [α]$_D$23: +175 (c = 0.11, CHCl$_3$). TLC (10% methanol in dichloromethane), Rf: 0.52 (UV, CAM, AgNO$_3$).

Synthesis of (3*R*,5a*S*,10b*S*,11a*R*)-3,11a-Dihydroxy-10b-(4-methoxyphenyl)-2,3-dimethyl-6-(phenylsulfonyl)-2,3,6,10b,11,11a-hexahydro-4*H*-pyrazino[1',2':1,5]pyrrolo[2,3-*b*]indole-1,4(5a*H*)-dione (38);[51] diol 38.

Bis(2,2'-bipyridyl)copper(II) permanganate[39] (1.61 g, 2.62 mmol, 2.70 equiv) was added as a solid to solution of anisole adduct (+)–**37** (502 mg, 0.970 mmol, 1 equiv) in dichloromethane (10 mL) at 23 °C. After 50 min, the reaction mixture was diluted with dichloromethane (100 mL) and was poured into an aqueous sodium bisulfite solution (1 M, 200 mL). The layers were separated, and the organic layer was washed sequentially with an aqueous sodium bisulfite solution (1 M, 75 mL), with a mixture of a saturated aqueous copper(II) sulfate solution and deionized water (1:1, 100 mL), with a saturated aqueous ammonium chloride solution (100 mL), and with a saturated aqueous sodium chloride solution (100 mL). The aqueous layers were separately extracted with dichloromethane (2 × 75 mL). The combined organic extracts were dried over anhydrous sodium sulfate, were filtered, and were concentrated under reduced pressure. The resulting light blue foam was purified by flash column chromatography on silica gel (eluent: 0→30% acetone in dichloromethane) to afford diol **38** (393 mg, 74%) as a white foam. 1H NMR (400 MHz,

CDCl$_3$, 25 °C): δ 7.61 (d, *J* = 8.1 Hz, 1H), 7.34–7.26 (m, 4H), 7.22–7.15 (m, 2H), 7.02 (app-t, *J* = 7.9 Hz, 2H), 6.78 (app-d, *J* = 8.9 Hz, 2H), 6.55 (app-d, *J* = 8.9 Hz, 2H), 6.35, (s, 1H), 5.62 (br-s, 1H), 5.24 (br-s, 1H), 3.76 (s, 3H), 3.38 (d, *J* = 15.1 Hz, 1H), 2.99 (s, 3H), 2.92 (d, *J* = 15.1 Hz, 1H), 1.81 (s, 3H). 13C{1H} NMR (100 MHz, CDCl$_3$, 25 °C): δ 168.2, 166.8, 158.4, 140.0, 138.2, 137.7, 133.9, 132.9, 129.1, 128.6, 128.5, 127.5, 126.5, 126.1, 118.0, 114.3, 88.7, 87.4, 85.7, 58.1, 55.4, 49.6, 28.1, 22.8. FTIR (thin film) cm^{-1}: 3375 (br), 3067 (w), 1687 (m), 1512 (m), 1361 (m), 1252 (m), 1169 (s), 832 (w), 737 (w), 600 (m). HRMS (ESI) *m/z*: [M + H]$^+$ calc'd for C$_{28}$H$_{28}$N$_3$O$_7$S 550.1642; Found 550.1640. TLC (20% acetone in dichloromethane), R*f*: 0.22 (UV, CAM).

Synthesis of Sodium 4-methoxybenzyl carbonotrithioate (39); monosodium trithiocarbonate 39.

A suspension of sodium hydride (60% dispersion, 1.03 g, 25.8 mmol, 1 equiv) in diethyl ether (125 mL) at 0 °C was sparged with argon for 20 min by discharge of a balloon equipped with a needle extending into the reaction mixture. *p*-Methoxybenzyl thiol (4.5 mL, 33 mmol, 1.3 equiv) was added dropwise via syringe over 2 min, the solution was stirred for 5 min, then the ice-water bath was removed and the reaction mixture was allowed to stir and warm to 23 °C. After 1 h, the light-gray suspension was cooled to 0 °C, and carbon disulfide (2.0 mL, 33 mmol, 1.3 equiv) was added dropwise via syringe over 3.5 min. The ice-water bath was removed and the reaction mixture was allowed to stir and warm to 23 °C. After 2 h, a yellow precipitate was collected by filtration of the yellow suspension through a 350-mL medium-porosity fritted-glass funnel. The yellow precipitate was washed with hexanes (2 × 50 mL) and was dried under reduced pressure to afford monosodium trithiocarbonate **39** (5.76 g, 88%) as a yellow solid. 1H NMR (500 MHz, DMSO-d$_6$, 25 °C): δ 7.20 (d, *J* = 8.6 Hz, 2H), 6.81 (d, *J* = 8.6 Hz, 2H), 4.29 (s, 2H), 3.71 (s, 3H). ^{13}C{^{1}H} NMR (125 MHz, DMSO-d$_6$, 25 °C): δ 239.0, 157.8, 130.9, 129.8, 113.5, 55.0, 44.6. FTIR (thin film) cm^{-1}: 1507 (w), 1248 (w), 1229 (w), 1177 (w), 1003 (s), 833 (m), 539 (m). HRMS (DART-TOF) *m/z*: [M − Na]$^-$ calc'd for C$_9$H$_9$OS$_3$ 228.9821; Found 228.9813.

Synthesis of (+)–(4*S*,6a*S*,11b*S*,12a*S*)-11b-(4-Methoxyphenyl)-4,14-dimethyl-7-(phenylsulfonyl)-2thioxo-6a,7,11b,12-tetrahydro-4,12a-(epiminomethano) [1,3,5]dithiazepino[5',4':1,5]pyrrolo[2,3-*b*]indole5,13(4*H*)-dione (41);[51] dithiepanethione (+)–41.

A mixture of regioisomeric silyl ethers23 **S15** and **S16** (1.1:1, 956 mg, 1.44 mmol, 1 equiv) was azeotropically dried by concentration from dichloromethane (5 mL) and anhydrous benzene (50 mL) under reduced pressure. The resulting white foam was dissolved in acetonitrile (100 mL) via cannula, and monosodium trithiocarbonate **39** (1.82 g, 7.21 mmol, 5.01 equiv) was added as a solid. Trifluoroacetic acid (TFA, 50 mL) was poured rapidly into the reaction mixture over 15 seconds, resulting in a homogeneous yellow solution. After 1 h, the dark orange solution was diluted with ethyl acetate-hexanes (9:1, 100 mL), was slowly poured into a saturated aqueous sodium bicarbonate solution (650 mL), and the biphasic mixture was stirred vigorously for 30 min. The aqueous layer was extracted with ethyl acetate-hexanes (9:1, 2 × 100 mL), and the combined organic extracts were washed sequentially with deionized water (200 mL) and with a saturated aqueous sodium chloride solution (150 mL). The combined aqueous layers were extracted with a single portion of

ethyl acetate-hexanes (4:1, 100 mL), and the combined organic extracts were dried over anhydrous sodium sulfate, were filtered, and were concentrated under reduced pressure. The resulting residue was purified by flash column chromatography on silica gel (eluent: 0→7.5% diethyl ether in dichloromethane) to afford dithiepanethione (+)–**41** (766 mg, 85%) as a yellow foam. ^{1}H NMR (400 MHz, CDCl$_3$, 25 °C): δ 7.55 (d, J = 8.1 Hz, 1H), 7.43 (app-d, J = 7.6 Hz, 2H), 7.30–7.21 (m, 2H), 7.30–7.21 (m, 2H), 7.13 (app-t, 2H), 6.87 (app-d, J = 8.8 Hz, 2H), 6.68 (app-d, J = 8.8 Hz, 2H), 6.59 (s, 1H), 3.78 (s, 3H), 3.53 (d, J = 15.3 Hz, 1H), 3.06 (s, 3H), 3.05 (d, J = 15.2 Hz, 1H), 1.92 (s, 3H). 13C{^{1}H} NMR (100 MHz, CDCl$_3$, 25 °C): δ 215.7, 164.7, 160.5, 159.0, 141.5, 138.9, 134.9, 133.1, 131.4, 130.1, 128.7, 127.5, 126.8, 126.4, 125.5, 118.7, 114.6, 87.8, 75.0, 73.5, 57.8, 55.5, 48.7, 28.4, 19.8. FTIR (thin film) cm^{-1}: 3002 (w), 1713 (s), 1685 (s), 1476 (w), 1362 (s), 1169 (s), 1034 (m), 999 (m), 895 (w), 737 (m), 599 (m). HRMS (ESI) m/z: [M + H]$^+$ calc'd for C$_{29}$H$_{26}$N$_3$O$_5$S$_4$ 624.0750; Found 624.0747. [α]$_D$23: +148 (c = 0.61, CHCl$_3$). TLC (5% diethyl ether in dichloromethane), Rf: 0.31 (UV, CAM, AgNO$_3$, DTNB).

Synthesis of (+)–(3*S*,5a*S*,10b*S*,11a*S*)-10b-(4-Methoxyphenyl)-2,3-dimethyl-6-(phenylsulfonyl)2,3,5a,6,10b,11-hexahydro-3,11a-epidithiopyrazino[1',2':1,5]pyrrolo[2,3-*b*]indole-1,4-dione (42);[51] epidithiodiketopiperazine (+)–42.

A yellow solution of dithiepanethione (+)–**41** (374 mg, 0.600 mmol, 1 equiv) in acetone (15 mL) at 23 °C was sparged with argon for 10 min by discharge of a balloon equipped with a needle extending into the reaction mixture. Ethanolamine (3.75 mL) was added via syringe over 30 seconds, resulting in a nearly colorless solution. After 1 h, the reaction mixture was diluted with ethyl acetate-hexanes (9:1, 100 mL) and was washed with an aqueous hydrogen chloride solution (1 M, 150 mL). The aqueous layer was extracted with ethyl acetate-hexanes (9:1, 2 × 50 mL), and the combined organic extracts were washed with a saturated aqueous sodium chloride solution (100 mL). A stock solution of potassium triiodide in pyridine was added dropwise into the organic layer containing crude bisthiol until a persistent yellow color was observed. The resulting mixture was washed sequentially with an aqueous hydrogen chloride solution (1 M, 2 × 75 mL), with a mixture of deionized water and a saturated aqueous sodium thiosulfate solution (3:1, 100 mL), with deionized water (100 mL), and with a saturated aqueous sodium chloride solution (100 mL). The aqueous layers were separately extracted with a single portion of ethyl acetate-hexanes (9:1, 100 mL). The combined organic extracts were dried over anhydrous sodium sulfate, were filtered, and were concentrated under reduced pressure. The resulting residue was purified by flash column chromatography on silica gel (eluent: 15% dichloromethane, 0→7.5% isopropanol in hexanes) to afford epidithiodiketopiperazine (+)–**42** (304 mg, 87%) as a white solid. 1H NMR (500 MHz, CDCl$_3$, 25 °C): δ 7.65 (d, J = 8.0 Hz, 1H), 7.40 (app-t, d, J = 7.1, 1.5 Hz, 1H), 7.34 (dd, J = 8.5, 1.2 Hz, 2H), 7.31–7.22 (m, 3H), 7.02 (app-t, J = 7.5 Hz, 2H), 6.74 (app-d, J = 8.8 Hz, 2H), 6.62 (app-d, J = 8.7 Hz, 2H), 6.42 (s, 1H), 3.79 (s, 3H), 3.67 (d, J = 15.6 Hz, 1H), 3.05 (s, 3H), 2.88 (d, J = 15.5 Hz, 1H), 1.97 (s, 3H). ^{13}C{^{1}H} NMR (100 MHz, CDCl$_3$, 25 °C): δ 165.8, 161.4, 158.8, 141.2, 138.3, 135.8, 132.9, 131.4, 129.7, 128.5, 127.9, 127.2, 126.1, 125.6, 119.0, 114.5, 88.0, 73.9, 73.5, 59.1, 55.5, 46.1, 27.6, 18.2. FTIR (thin film) cm^{-1}: 2951 (br), 2359 (w), 1679 (s), 1514 (s), 1457 (m), 1341 (s), 1249 (s), 1163 (s), 1028 (m), 905 (m), 730 (s). HRMS (ESI) m/z: [M + H]$^+$ calc'd for

$C_{28}H_{26}N_3O_5S_3$ 580.1029; Found 580.1032. $[\alpha]_D23$: +293 (c = 0.57, CHCl₃). TLC (15% dichloromethane and 15% isopropanol in hexanes), Rf: 0.42 (UV, CAM, AgNO₃).

Synthesis of (3*S*,5a*S*,10b*S*,11a*S*)-3,11a-Bis((4-fluorobenzyl)disulfaneyl)-10b-(4-methoxyphenyl)-2,3dimethyl-6-(phenylsulfonyl)-2,3,6,10b,11,11a-hexahydro-4*H*-pyrazino[1',2':1,5]pyrrolo[2,3-*b*]indole-1,4(5a*H*)-dione (45a);[51] bis(*p*-fluorobenzyl)disulfide 45a.

Triethylamine (70 μL, 0.50 mmol, 2.5 equiv) and (*p*-fluorophenyl)methanethiol (PFB-SH, 25 μL, 0.20 mmol, 1.0 equiv) were added via syringe to a solution of epidithiodiketopiperazine (+)−**42** (116 mg, 0.200 mmol, 1 equiv) and 1,2-bis(*p*-fluorobenzyl)disulfane (PFB-SSPFB, 552 mg, 1.95 mmol, 9.75 equiv) in tetrahydrofuran (0.5 mL) at 23 °C. After 15 h, additional tetrahydrofuran (1.1 mL) was added via syringe to dissolve a white precipitate. After an additional 50 h, the reaction mixture was concentrated under reduced pressure and the resulting residue was purified by flash column chromatography on silica gel (eluent: 0→15% ethyl acetate in dichloromethane) to afford bisdisulfide **45a** (38.7 mg, 22.4%) as a white solid and recovered epidithiodiketopiperazine (+)−**42** (76.6 mg, 66%) as a white solid. 1H NMR (400 MHz, CDCl₃, 25 °C): δ 7.67 (d, *J* = 8.1 Hz, 1H), 7.48 (app-d, *J* = 7.6 Hz, 2H), 7.38–7.33 (m, 3H), 7.30 (app-t, *J* = 7.7 Hz, 1H), 7.22–7.15 (m, 2H), 7.14–7.09 (m, 4H), 6.95 (app-t, *J* = 8.7 Hz, 2H), 6.90 (app-t, *J* = 8.6 Hz), 6.67 (app-d, *J* = 8.8 Hz, 2H), 6.59 (s, 1H), 6.58 (app-d, *J* = 9.1 Hz, 2H), 4.09 (d, *J* = 12.9 Hz, 1H), 3.99 (d, *J* = 12.9 Hz, 1H), 3.84 (d, *J* = 14.7 Hz, 1H), 3.83 (s, 2H), 3.76 (s, 3H), 3.10 (s, 3H), 2.99 (d, *J* = 14.8 Hz, 1H), 2.09 (s, 3H). ¹³C{¹H} NMR (100 MHz, CDCl₃, 25 °C): δ 167.4, 164.2, 162.3 (d, *J* = 245.6 Hz), 162.3 (d, *J* = 246.3 Hz), 158.6, 142.2, 137.9, 135.5, 133.2, 133.1, 132.9 (d, *J* = 3.2 Hz), 132.4 (d, *J* = 3.3 Hz), 131.7 (d, *J* = 8.2 Hz), 131.3 (d, *J* = 8.2 Hz), 129.4, 128.7, 127.5, 127.5, 125.9, 125.7, 118.5, 115.5 (d, *J* = 21.5 Hz), 115.4 (d, *J* = 21.5 Hz), 114.3, 88.3, 73.7, 71.1, 57.1, 55.5, 46.9, 42.2, 41.7, 29.5, 22.8. FTIR (thin film) cm⁻¹: 3485 (br), 2927 (br), 2106 (w), 1663 (m), 1600 (w), 1509 (s), 1362 (s), 833 (m), 687 (w), 599 (m). HRMS (ESI) *m/z*: [M + H]⁺ calc'd for $C_{42}H_{38}F_2N_3O_5S_5$ 862.1378; Found 862.1371. TLC (5% ethyl acetate in dichloromethane), Rf: 0.35 (UV, CAM, AgNO₃).

Synthesis of Triethylammonium *S*-(((3*S*,5a*S*,10b*S*,11a*S*)-3-(((*R*)-2-((*S*)-4-amino-4-carboxybutanamido)-3-((carboxymethyl)amino)-3-oxopropyl)disulfaneyl)-10b-(4-methoxyphenyl)-2,3-dimethyl-1,4-dioxo-6-(phenylsulfonyl)-1,2,3,4,5a,6,10b,11-octahydro-11a*H*-pyrazino[1',2':1,5]pyrrolo[2,3-*b*]indol-11a-yl)thio)*N*-((*S*)-4-amino-4-carboxybutanoyl)-*L*-cysteinylglycinate (46);[51] bis(L-glutathione)disulfide 46.

Sodium borohydride (4.9 mg, 0.13 mmol, 4.3 equiv) was added as a solid in one portion to a solution of epidithiodiketopiperazine (+)−**42** (17.3 mg, 29.8 μmol, 1 equiv) in tetrahydrofuran (4.0 mL) and methanol (30 μL). After 35 min, the reaction mixture was diluted with ethyl acetate-hexanes (9:1, 40 mL) and was washed sequentially with a saturated aqueous ammonium chloride solution (40 mL), with deionized water (30 mL), and with a saturated aqueous sodium chloride solution (20 mL). The aqueous layers were separately extracted with a single portion of ethyl acetate-hexanes (9:1, 25 mL). The combined organic extracts were dried over anhydrous sodium sulfate, were filtered, and were sparged with argon for 15 min by discharge of a balloon equipped with a needle extending into the stirring reaction mixture. The reaction mixture was then concentrated

under reduced pressure, and the resulting residue containing bisthiol was dissolved in tetrahydrofuran (0.25 mL) and added dropwise via syringe to a solution of *S*-(phenylsulfonyl)-L-glutathione hydrogen chloride[44] (72.9 mg, 163 μmol, 5.45 equiv) and triethylamine (45 μL, 320 μmol, 11 equiv) in tetrahydrofuran (1.1 mL) and methanol (1.1 mL). The transfer was quantitated with additional tetrahydrofuran (2 × 0.25 mL). After 19 h, the reaction mixture was diluted with methanol and adsorbed onto diatomaceous earth (0.4 g) by concentration under reduced pressure until a free-flowing powder was obtained. The diatomaceous earth-absorbed crude mixture was purified by flash column chromatography on C_{18}-reversed phase silica gel (eluent: 10→80% acetonitrile in water) to afford the bisdisulfide **46** (17.2 mg, 45%) as a white solid and recovered epidithiodiketopiperazine (+)−**42** (6.0 mg, 21%). 1H NMR (500 MHz, 5:1 D_2O:CD_3CN, 25 °C): δ 7.45 (d, *J* = 8.2 Hz, 1H), 7.42–7.34 (m, 3H), 7.32 (app-t, *J* = 7.7 Hz, 1H), 7.26 (d, *J* = 7.6 Hz, 1H), 7.16 (app-t, *J* = 7.5 Hz, 1H), 7.10 (app-t, *J* = 7.8 Hz, 2H), 6.70 (app-d, *J* = 8.4 Hz, 2H), 6.59 (app-d, *J* = 8.4 Hz, 2H), 6.40 (s, 1H), 4.66 (dd, *J* = 8.6, 5.1 Hz, 1H), 4.42 (dd, *J* = 10.0, 4.0 Hz, 1H), 3.80–3.57 (m, 9H), 3.54 (d, *J* = 14.6 Hz), 3.26–3.03 (m, 9H), 3.03–2.93 (m, 4H), 2.65–2.54 (m, 1H), 2.42 (app-t, *J* = 7.6 Hz, 2H), 2.34 (app-t, *J* = 7.7 Hz, 2H), 2.04 (app-q, *J* = 7.2 Hz, 2H), 1.98 (app-q, *J* = 7.5 Hz, 2H), 1.89 (s, 3H), 1.17 (t, *J* = 7.3 Hz, 9H). $^{13}C\{^1H\}$ NMR (125 MHz, 5:1 D_2O:CD_3CN, 25 °C): δ 174.5 (br, 2C), 173.7, 173.6, 172.8, 170.5, 170.0, 166.6, 163.9, 157.0, 140.3, 135.6, 134.7, 133.5, 132.3, 128.8, 128.4, 126.7, 125.9, 125.6, 125.3, 117.3, 113.7, 87.1, 73.1, 71.5, 56.1, 54.6, 53.3, 53.2, 52.1, 51.7, 45.8, 44.4, 42.3, 42.2, 40.4, 37.5, 30.8, 30.7, 29.2, 25.5, 25.4, 20.8, 7.4. FTIR (thin film) cm^{-1}: 3273 (br), 1645 (s), 1513 (s), 1253 (m), 1167 (m), 1109 (w), 1028 (w), 832 (w), 686 (m). HRMS (ESI) *m/z*: [M + Na]$^+$ calc'd for $C_{48}H_{57}N_9NaO_{17}S_5$ 1214.2368; Found 1214.2359. TLC (30% acetonitrile in water, C_{18}-reversed phase), R*f*: 0.25 (UV, CAM, $AgNO_3$).

Synthesis of *tert*-Butyl (2-(2-(2-((1-(3-(4-((3*S*,5a*S*,10b*S*,11a*S*)-2,3-dimethyl-1,4-dioxo-6(phenylsulfonyl)-1,2,3,4,5a,6-hexahydro-3,11a-epidithiopyrazino[1',2':1,5]pyrrolo[2,3-*b*]indol-10b(11*H*)yl)phenoxy)propyl)-1*H*-1,2,3-triazol-4-yl)methoxy)ethoxy)ethoxy)ethyl)carbamate;[51] triazole 51.

A solution of *N,N*-diisopropylethylamine (DIPEA, 2.7 μL, 16 μmol, 1.5 equiv) and acetic acid (AcOH, 0.90 μL, 16 μmol, 1.5 equiv) in toluene (0.2 mL) was added to a flask containing azide (+)−**9d** (6.8 mg, 11 μmol, 1 equiv) and alkyne[23] **50** (11.6 mg, 40.4 μmol, 3.67 equiv). Copper (I) iodide (0.9 mg, 5 μmol, 0.5 equiv) was added as a solid, and the suspension was sparged with argon for 2 min by discharge of balloon equipped with a needle extending into the reaction mixture. After 17 h, the reaction mixture was diluted with dichloromethane (0.5 mL) and was purified by flash chromatography on silica gel (eluent: 5→40% acetone in dichloromethane) to afford triazole **51** as a yellow solid. The mixture was further purified by flash column chromatography on silica gel (eluent: 0→4% methanol in dichloromethane) to afford triazole **51** (9.0 mg, 92%) as a white solid. 1H NMR (500 MHz, CDCl$_3$, 25 °C): δ 7.68–7.60 (m, 2H), 7.40 (app-t, *J* = 7.6 Hz, 1H), 7.36 (app-d, *J* = 7.9 Hz, 2H), 7.31 (app-t, *J* = 7.5 Hz, 1H), 7.29–7.22 (m, 2H), 7.05 (app-t, *J* = 7.7 Hz, 2H), 6.74 (app-d, *J* = 8.2 Hz, 2H), 6.59 (br-s, 2H), 6.42 (s, 1H), 5.04 (br-s, 1H), 4.70 (s, 2H), 4.60 (t, *J* = 5.7 Hz, 2H), 3.97–3.88 (m, 2H), 3.73–3.57 (m, 9H), 3.53 (t, *J* = 5.0 Hz, 2H), 3.30 (app-q, *J* = 5.5 Hz, 2H), 3.05 (s, 3H), 2.88 (d, *J* = 15.5 Hz, 1H), 2.40 (p, *J* = 6.4 Hz, 2H), 1.96 (s, 3H), 1.43 (s, 9H). 13C{1H} NMR (125 MHz, CDCl$_3$, 25 °C): δ 165.8, 161.4, 157.7, 156.1,

145.5, 141.3, 138.5, 135.8, 133.1, 132.0, 129.8, 128.6, 128.0, 127.2, 126.1, 125.5, 123.0, 119.0, 115.0, 87.9, 79.3, 73.9, 73.5, 70.7 (3C), 70.4, 69.9, 64.8, 64.2, 59.1, 47.1, 46.0, 40.5, 30.0, 28.6 (3C), 27.7, 18.2. FTIR (thin film) cm^{-1}: 3360 (br-m), 2921 (s), 2851 (m), 1659 (m), 1632 (m), 1468 (w), 1411 (w), 1024 (w), 801 (w). HRMS (ESI) m/z: [M + Na]$^+$ calc'd for $C_{44}H_{53}N_7NaO_{10}S_3$ 958.2908; Found 958.2902. TLC (5% methanol in dichloromethane), Rf: 0.26 (UV, CAM, AgNO$_3$).

Cell Culture Information.

Cells were grown in media supplemented with fetal bovine serum (FBS) and antibiotics (100 µg/mL penicillin and 100 U/mL streptomycin). Specifically, experiments were performed using the following cell lines and media compositions: HeLa (cervical adenocarcinoma) and A549 (lung carcinoma) were grown in RPMI-1640 + 10% FBS; HCT 116 (colorectal carcinoma) was grown in DMEM + 10% FBS; MCF7 (breast adenocarcinoma) and DU 145 (prostate carcinoma) were grown in EMEM + 10% FBS. Cells were incubated at 37 °C in a 5% CO$_2$, 95% humidity atmosphere.

Cell Viability Assays.

Cells were plated at 250 cells/well into duplicate assay plates in 50 µL media into 384well white, opaque, tissue-culture treated plates and allowed to adhere overnight at 37 °C/5% CO$_2$. Compounds were solubilized in DMSO as 1000× stocks and 100 nL was pin-transferred to cells. Compounds were tested in 10pt, 2-fold dilution with concentrations tested between 1 nM – 20 µM for most compounds, except where indicated. DMSO (32 wells of 384-wells) was used as vehicle control. After 72 hours of incubation at 37 °C/5% CO$_2$, 10 µL Cell Titer-Glo was added to each well and plates were incubated at room temperature for 10 minutes before the luminescence was read on a plate reader. Cell Titer-Glo measures ATP levels of cells as a surrogate for cell viability. All compound-treated wells were normalized to the DMSO control averages and expressed as a % of DMSO viability. IC$_{50}$ values were determined from the dose curves using Spotfire.

Supplementary Material

Refer to Web version on PubMed Central for supplementary material.

ACKNOWLEDGMENTS

REFERENCES

(1). (a)For reviews on epipolythiodiketopiperazines, see:Hino T and Nakagawa M, in The Alkaloids: Chemistry and Pharmacology, ed. Brossi A, Academic Press, New York, 1989, vol. 34, ch. 1, pp. 1–75.(b)Gardiner DM; Waring P; Howlett BJ The Epipolythiodioxopiperazine (ETP) Class of Fungal Toxins: Distribution, Mode of Action, Functions and Biosynthesis. Microbiology, 2005, 151, 1021–1032. [PubMed: 15817772] (c)Jiang C-S; Guo Y-W Epipolythiodioxopiperazines from Fungi: Chemistry and Bioactivities. Mini-Rev. Med. Chem 2011, 9, 728–745.
(2). Kim J; Movassaghi M Biogenetically-Inspired Total Synthesis of Epidithiodiketopiperazines and Related Alkaloids. Acc. Chem. Res 2015, 48, 1159–1171. [PubMed: 25843276]

(3). Kim J; Movassaghi M Biogenetically Inspired Syntheses of Alkaloid Natural Products. Chem. Soc. Rev 2009, 38, 3035–3050. [PubMed: 19847339]

(4). Boyer N; Morrison KC; Kim J; Hergenrother PJ; Movassaghi M Synthesis and Anticancer Activity of Epipolythiodiketopiperazine Alkaloids. Chem. Sci 2013, 4, 1646–1657. [PubMed: 23914293]

(5). (a)For representative anticancer activity of epipolythiodiketopiperazines, see:Vigushin DM; Mirsaidi N; Brooke G; Sun C; Pace P; Inman L; Moody CJ; Coombes RC Gliotoxin is a Dual Inhibitor of Farnesyltransferase and Geranylgeranylteransferase I with Antitumor Activity Against Breast Cancer In Vivo. Med. Oncol 2004, 21, 21–30. [PubMed: 15034210] (b)Isham CR; Tibodeau JD; Jin W; Xu R; Timm MM; Bible KC Chaeotocin: A Promising New Antimyeloma Agent with *in vitro* and *in vivo* Activity Mediated via Imposition of Oxidative Stress. Blood 2007, 109, 2579–2588. [PubMed: 17090648] (c)Cook KM; Hilton ST; Mecinovi J; Motherwell WB; Figg WD; Schofield CJ Epidithiodiketopiperazines Block the Interaction between Hypoxia-Inducible-Factor1α(HIF-1α) and p300 by a Zinc Ejection Mechanism. J. Biol. Chem 2009, 39, 26831–26838.(d)Liu F; Liu Q; Yang D; Bollag WB; Roberston K; Wu P; Liu K Verticillin A Overcomes Apoptosis Resistance in Human Colon Carcinoma Through DNA Methylation-Dependent Upregulation of BNIP3. Cancer Res. 2011, 71, 6807–6816. [PubMed: 21911457] (e)Dubey R; Levin MD; Szabo LZ; Laszlo CF; Kushal S; Singh JB; Oh P; Schnitzer JE; Olenyuk BZ Suppression of Tumor Growth by Designed Dimeric Epidithiodiketopiperazine Targeting Hypoxia-Inducible Transcription Factor Complex. J. Am. Chem. Soc 2013, 135, 4537–4549. [PubMed: 23448368] (f)Dewangan J; Srivastava S; Mishra S; Pandey PK; Divakar A; Rath SK Chetomin Induces Apoptosis in Human TripleNegative Breast Cancer Cells by Promoting Calcium Overload and Mitochondrial Dysfunction. Biochem. Biophys. Res. Commun 2018, 495, 1915–1921, and references cited therein. [PubMed: 29208466]

(6). For antifungal activity of epipolythiodiketopiperazines, see Saleh AA; Jones GW; Tinley FC; Delaney SF; Alabbadi SH; Fenlon K; Doyle S; Owens RA Systems Impact of Zinc Chelation by the Epipolythiodioxopiperazine Dithiol Gliotoxin in *Aspergillus fumigatus*: A New Direction in Natural Product Functionality. Metallomics 2018, 10, 854–866. [PubMed: 29897360]

(7). For antibacterial activity of epipolythiodiketopiperazines, see Zheng C-J; Kim C-J; Bae KS; Kim Y-H; Kim W-G Bionectins A–C, Epidithiodioxopiperazines with Anti-MRSA Activity, from *Bionectra byssicola* F120. J. Nat. Prod 2006, 69, 1816–1819. [PubMed: 17190469]

(8). For antiviral activity of epipolythiodiketopiperazines, see Asquith CRM; Sil BC; Laitinen T; Tizzard GJ; Coles SJ; Poso A; Hofmann-Lehmann R; Hilton ST Novel Epidithiodiketopiperazines as Anti-Viral Zinc Ejectors of the Feline Immunodeficiency Virus (FIV) Nucleocapsid Protein as a Model for HIV Infection. Bioorg. Med. Chem 2019, 27, 4174–4184. [PubMed: 31395510]

(9). (a)For representative syntheses of epipolythiodiketopiperazines from our laboratory, see:Kim J; Ashenhurst JA; Movassaghi M Total Synthesis of (+)−11,11′-Dideoxyverticillin A. Science 2009, 324, 238–241. [PubMed: 19359584] (b)Kim J; Movassaghi M General Approach to Epipolythiodiketopiperazine Alkaloids: Total Synthesis of (+)−Chaetocins A and C and (+)−12,12′-Dideoxychetracin A. J. Am. Chem. Soc 2010, 132, 14376–14378. [PubMed: 20866039] (c)Coste A; Kim J; Adams TC; Movassaghi M Concise Total Synthesis of (+)Bionectins A and C. Chem. Sci 2013, 4, 3191–3197. [PubMed: 23878720]

(10). (a)For representative syntheses of epipolythiodiketopiperazines, see:Fukuyama T; Nakatsuka S-I; Kishi Y Total Synthesis of Gliotoxin, Dehydrogliotoxin, and Hyalodendrin. Tetrahedron 1981, 37, 2045–2078.(b)Overman LE; Sato T Construction of Epidithiodioxopiperazines by Directed Oxidation of Hydroxyproline-Derived Dioxopiperazines. Org. Lett 2007, 9, 5267–5270. [PubMed: 18001051] (c)Iwasa E; Hamashima Y; Fujishiro S; Higuchi E; Ito A; Yoshida M; Sodeoka M Total Synthesis of (+)−Chaetocin and its Analogues: Their Histone Methyltransferase G9a Inhibitory Activity. J. Am. Chem. Soc 2010, 132, 4078–4079. [PubMed: 20210309] (d)Codelli JA; Puchlopek ALA ; Reisman SE Enantioselective Total Synthesis of (–)-Acetylaranotin, a Dihydrooxepine Epidithiodiketopiperazine. J. Am. Chem. Soc 2012, 134, 1930–1933. [PubMed: 22023250] (e)Takeuchi R; Shimokawa J; Fukuyama T Development of a Route to Chiral Epidithiodioxopiperazine Moieties and Application to the Asymmetric Synthesis of (+)−Hyalodendrin. Chem. Sci 2014, 5, 2003–2006.(f)Baumann M; Dieskau AP; Loertscher BM; Walton MC; Nam S; Xie J; Horne D; Overman LE Tricyclic Analogues of Epidithiodioxopiperazine Alkaloids with Promising *in vitro* and *in vivo* Antitumor Activity.

Chem. Sci 2015, 6, 4451–4457. [PubMed: 26301062] (g)Snaddon TN; Scaggs TD; Pearson CM; Fyfe JWB A Modular Construction of Epidithiodiketopiperazines. Org. Lett 2019, 21, 4873–4877. [PubMed: 31184903]

(11). (a)Bunnage ME; Chekler ELP; Jones LH Target Validation Using Chemical Probes. Nat. Chem. Biol 2013, 9, 195–199. [PubMed: 23508172] (b)Wright MH; Sieber SA Chemical Proteomics Approaches for Identifying the Cellular Targets of Natural Products. Nat. Prod. Rep 2016, 33, 681–708. [PubMed: 27098809]

(12). (a)Flygare JA; Pillow TH; Aristoff P Antibody-Drug Conjugates for the Treatment of Cancer. Chem. Biol. Drug Des 2013, 81, 113–121. [PubMed: 23253133] (b)Chari RVJ; Miller ML; Widdison WC Antibody-Drug Conjugates: An Emerging Concept in Cancer Therapy. Angew. Chem., Int. Ed 2014, 53, 3796–3827.(c)Beck A; Goetsch L; Dumontet C; Corvaïa N Strategies and Challenges for the Next Generation of Antibody–Drug Conjugates. Nat. Rev. Drug Discovery 2017, 16, 315–337. [PubMed: 28303026] (d)Birrer MJ; Moore KN; Betella I; Bates RC Antibody-Drug Conjugate-Based Therapeutics: State of the Science. J. Natl. Cancer Inst 2019, 111, 538–549. [PubMed: 30859213]

(13). Son BW; Jensen PR; Kauffman CA; Fenical W New Cytotoxic Epidithiodioxopiperazines Related to Verticillin A from a Marine Isolate of the Fungus Penicillium. Nat. Prod. Res 1999, 13, 213–222.

(14). The increased potency of N1-sulfonyl derivatives may be due to enhanced stability of the disulfide bridge or reduced metabolic degradation.

(15). The advantages include bypassing N-methylation of a complex DKP and more favorable reactivity differences at C11 vs. C15 hemiaminals, facilitating regio- and stereoselective DKP-sulfidation.

(16). (a)Rostovsev VV; Green LG; Fokin VV; Sharpless KB A Stepwise Hüisgen Cycloaddition Process: Copper(I)-Catalyzed Regioselective "Ligation" of Azides and Terminal Alkynes. Angew. Chem., Int. Ed 2002, 41, 2596–2599.(b)Hein JE; Fokin VV Copper-catalyzed Azide-Alkyne Cycloaddition (CuAAC) and Beyond: New Reactivity of Copper(I) Acetylides. Chem. Soc. Rev 2010, 39, 1302–1315. [PubMed: 20309487]

(17). Szpilman AM; Carreira EM Probing the Biology of Natural Products: Molecular Editing by Diverting Total Synthesis. Angew. Chem., Int. Ed 2010, 49, 9592–9628.

(18). (a)Cravatt BF; Wright AT; Kozarich JW; Activity-Based Protein Profiling: From Enzyme Chemistry to Proteomic Chemistry. Annu. Rev. Biochem 2008, 77, 383–414. [PubMed: 18366325] (b)Fonovi M; Bogyo M Activity-based Probes as a Tool for Functional Proteomic Analysis of Proteases. *Expert Rev.* Proteomics 2014, 5, 721–730.

(19). (a)Smith E; Collins I Photoaffinity Labeling in Target- and Binding-site Identification. Future Med. Chem 2015, 7, 159–183. [PubMed: 25686004] (b)Lapinsky DJ; Johnson DS Recent Developments and Applications of Clickable Photoprobes in Medicinal Chemistry and Chemical Biology. Future Med. Chem 2015, 7, 2143–2171. [PubMed: 26511756]

(20). Ghosh B; Jones LH Target Validation Using In-Cell Small Molecular Clickable Imaging Probes. Med. Chem. Commun 2014, 5, 247–254.

(21). Larson N; Ghandehari H Polymeric Conjugates for Drug Delivery. Chem. Mater 2012, 24, 840–853. [PubMed: 22707853]

(22). For a study employing a non-toxic ETP with an activated ester, see Zong L; Bartolami E; Abegg D; Adibekian A; Sakai N; Matile S Epidithiodiketopiperazines: Strain-Promoted Thiol-Mediated Cellular Uptake at the Highest Tension. ACS Cent. Sci 2017, 3, 449–453. [PubMed: 28573207]

(23). See the Supporting Information for further details.

(24). Kim J; Movassaghi M Concise Total Synthesis and Stereochemical Revision of (+)−Naseseazines A and B: Regioselective Arylative Dimerization of Diketopiperazine Alkaloids. J. Am. Chem. Soc 2011, 133, 14940–14943. [PubMed: 21875056]

(25). Unveiling of the primary alcohol using tetra-n-butylammonium fluoride in THF at 0 °C afforded an inseparable mixture of alcohol (+)−12 and its C11-epimer (3:1, respectively) in 88% yield.

(26). Lal B; Pramanik BN; Manhas MS; Bose AK Diphenylphosphoryl Azide: A Novel Reagent for the Stereospecific Synthesis of Azides from Alcohols. Tetrahedron Lett. 1977, 18, 1977–1980.

(27). (a)For our mechanistic studies of permanganate-promoted DKP-dihydroxylation, see:Bischoff AJ; Nelson BM; Niemeyer ZL; Sigman MS; Movassaghi M Quantitative Modeling of Bis(pyridine)silver(I) Permanganate Oxidation of Hydantoin Derivatives: Guidelines for Predicting the Site of Oxidation in Complex Substrates. J. Am. Chem. Soc 2017, 139, 15539–15547. [PubMed: 28975782] (b)Haines BE; Nelson BM; Grandner JM; Kim J; Houk KN; Movassaghi M; Musaev DG Mechanism of Permanganate-Promoted Dihydroxylation of Complex Diketopiperazines: Critical Roles of Counter-Cation and Ion-Pairing. J. Am. Chem. Soc 2018, 140, 13375–13386. [PubMed: 30295476]

(28). Karaman H; Barton RJ; Robertson BE; Lee DG Preparation and Properties of Quaternary Ammonium and Phosphonium Permanganates. J. Org. Chem 1984, 49, 4509–4516.

(29). Movassaghi M; Schmidt MA; Ashenhurst JA Concise Total Synthesis of (+)−WIN 64821 and (−)-Ditryptophenaline. Angew. Chem., Int. Ed 2008, 47, 1485–1487.

(30). Exposure of alkyne (+)−23 to palladium on carbon (Pd/C, 5 wt.%) and dihydrogen in ethyl acetate at 23 °C for 24 h gave an equimolar mixture of alcohol (+)−24 and the hydrogenated side product possessing the benzyloxy group, whereas otherwise identical treatment in ethanol provided alcohol (+)−24 (67%) alongside a deoxygenated N14-*n*-butyl side product (18%).

(31). Shao C; Wang X; Zhang Q; Luo S; Zhao J; Hu Y Acid–Base Jointly Promoted Copper(I)-Catalyzed Azide-Alkyne Cycloaddition. J. Org. Chem 2011, 76, 6832–6836. [PubMed: 21793533]

(32). Use of dichloromethane and toluene as solvent in the CuAAC reaction of ETP (+)−9c and alkyne 27 afforded ETP-triazole (+)28c in 73% and 85% yield, respectively.

(33). Reduction of the azide linker to the corresponding amine or early introduction of a *N*-Boc amine linker is not optimal given the sensitivity of the epidisulfide functional group and the conditions needed for accessing it.

(34). Thompson L; Ellman JA Synthesis and Applications of Small Molecule Libraries. Chem. Rev 1996, 96, 555–600. [PubMed: 11848765]

(35). Stephanopoulos N; Francis MB Choosing an Effective Protein Bioconjugation Strategy. Nat. Chem. Biol 2011, 7, 876–884. [PubMed: 22086289]

(36). Barré A; Tîntas M-L; Levacher V; Papamicaël C; Gembus V An Overview of the Synthesis of Highly Versatile *N*-Hydroxysuccinimide Esters. Synthesis 2017, 49, 472–483.

(37). Janes KA An Analysis of Critical Factors for Quantitative Immunoblotting. Sci. Signaling 2015, 8, pp. rs2.

(38). The structures of triketopiperazines 34b and 35b were confirmed through independent synthesis.

(39). Firouzabadi H; Sardarian AR; Naderi M; Vessal B Bis(2,2′-bipyridyl)-copper(II) Permanganate (BBCP): A Msild and Versatile Oxidant in Organic Synthesis. Tetrahedron 1984, 40, 5001–5004.

(40). The oxidation of C3-adduct (+)−37 with bis(pyridine)silver(I) permanganate gave diol 38 in 50–65% yield as a mixture of diastereomers (10:1 to 5:1), whereas the oxidation with tetra-n-butylammonium permanganate gave a complex mixture.

(41). (a)Chai CLL; Waring P Redox Sensitive Epidithiodioxopiperazines in Biological Mechanisms of Toxicity. Redox Rep. 2000, 5, 257–264. [PubMed: 11145100] (b)Srinivasan U; Bala A; Jao S-C; Starke DW; Jordan TW; Mieyal JJ Selective Inactivation of Glutaredoxin by Sporidesmin and Other Epidithiopiperazinediones. Biochemistry 2006, 45, 8978–8987. [PubMed: 16846241] (c)Bertling A; Niemann S; Uekötter A; Fegeler W; Lass-Flörl C; von Eiff C; Kehrel BE *Candida albicans* and its Metabolite Gliotoxin Inhibit Platelet Function via Interaction with Thiols. J. Thromb. Haemostasis 2010, 104, 270–278.

(42). (a)Bernardo PH; Chai CLL; Deeble GJ; Liu X-M; Waring P Evidence for Gliotoxin–Glutathione Conjugate Adducts. Bioorg. Med. Chem. Lett 2001, 11, 483–485. [PubMed: 11229753] (b)Bernardo PH; Brasch N; Chai CLL; Waring P; A Novel Redox Mechanism for the Glutathione-dependent Reversible Uptake of a Fungal Toxin In Cells. J. Biol. Chem 2003, 278, 46549–46555. [PubMed: 12947114]

(43). The isolation of bisdisulfide 45b was capricious due to its high reactivity in the presence of base and poor stability.

(44). Hart TW Some Observations Concerning the S-Nitroso and S-phenylsulphonyl Derivatives of L-Cysteine and Glutathione. Tetrahedron Lett. 1985, 26, 2013–2016.

(45). As ETP(+)–42 is insoluble in deuterium oxide, it was necessary to include deuteroacetonitrile to monitor the reversion of bisdisulfide 46 to ETP (+)–42.

(46). Szajewski RP; Whitesides GM Rate Constants and Equilibrium Constants for Thiol-Disulfide Interchange Reactions Involving Oxidized Glutathione. J. Am. Chem. Soc 1980, 102, 2011–2026.

(47). (a)Ramirez A; Ramadan B; Ritzenthaler JD; Rivera HN; Jones DP; Roman J Extracellular Cysteine/Cystine Redox Potential Controls Lung Fibroblast Proliferation and Matrix Expression through Upregulation of Transforming Growth Factor-Beta. Am. J. Physiol.: Lung Cell. Mol. Physiol 2007, 293, 972–981.(b)Chaiswing L; Zhong W; Cullen JJ; Oberley LW; Oberley TD Extracellular Redox State Regulates Features Associated with Prostate Cancer Cell Invasion. Cancer Res. 2008, 68, 5820–5826. [PubMed: 18632636]

(48). Still WC; Kahn M; Mitra A Rapid Chromatographic Technique for Preparative Separations with Moderate Resolution. J. Org. Chem 1978, 43, 2923–2925.

(49). Murdock KC Antiviral Agents. Chemical Modifications of a Disulfide Antibiotic, Acetylaranotin. J. Med. Chem 1974, 17, 827–835. [PubMed: 4602597]

(50). Fulmer GR; Miller AJM; Sherden NH; Gottlieb HE; Nudelman A; Stoltz BM; Bercaw JE; Goldberg KI NMR Chemical Shifts of Trace Impurities: Common Laboratory Solvents, Organics, and Gases in Deuterated Solvents Relevant to the Organometallic Chemist. Organometallics 2010, 29, 2176–2179.

(51). Per *Journal of Organic Chemistry* requirement, we have provided the systematic compound names following the International Union of Pure and Applied Chemistry (IUPAC) convention. For a complementary unified numbering system used throughout this report for comparison with related compounds, see Figure S1.
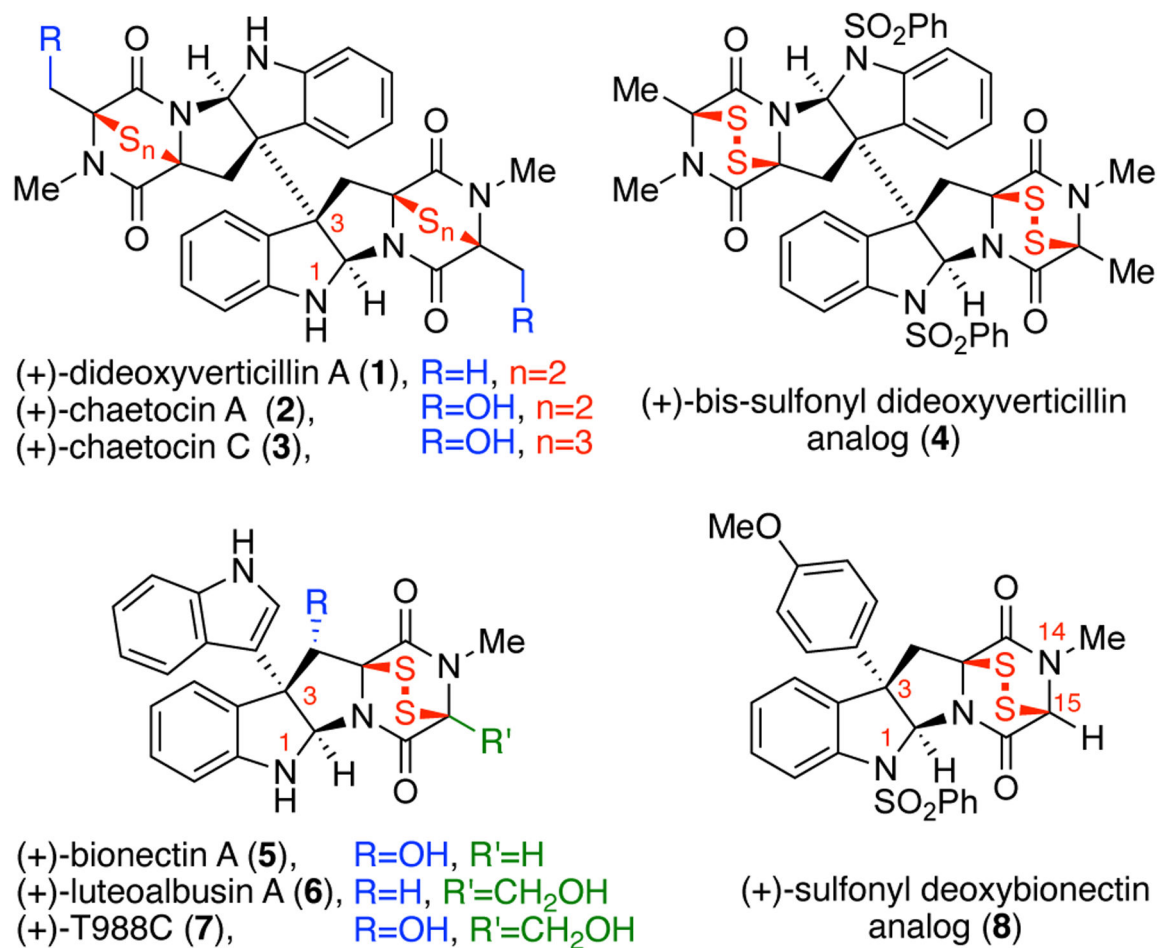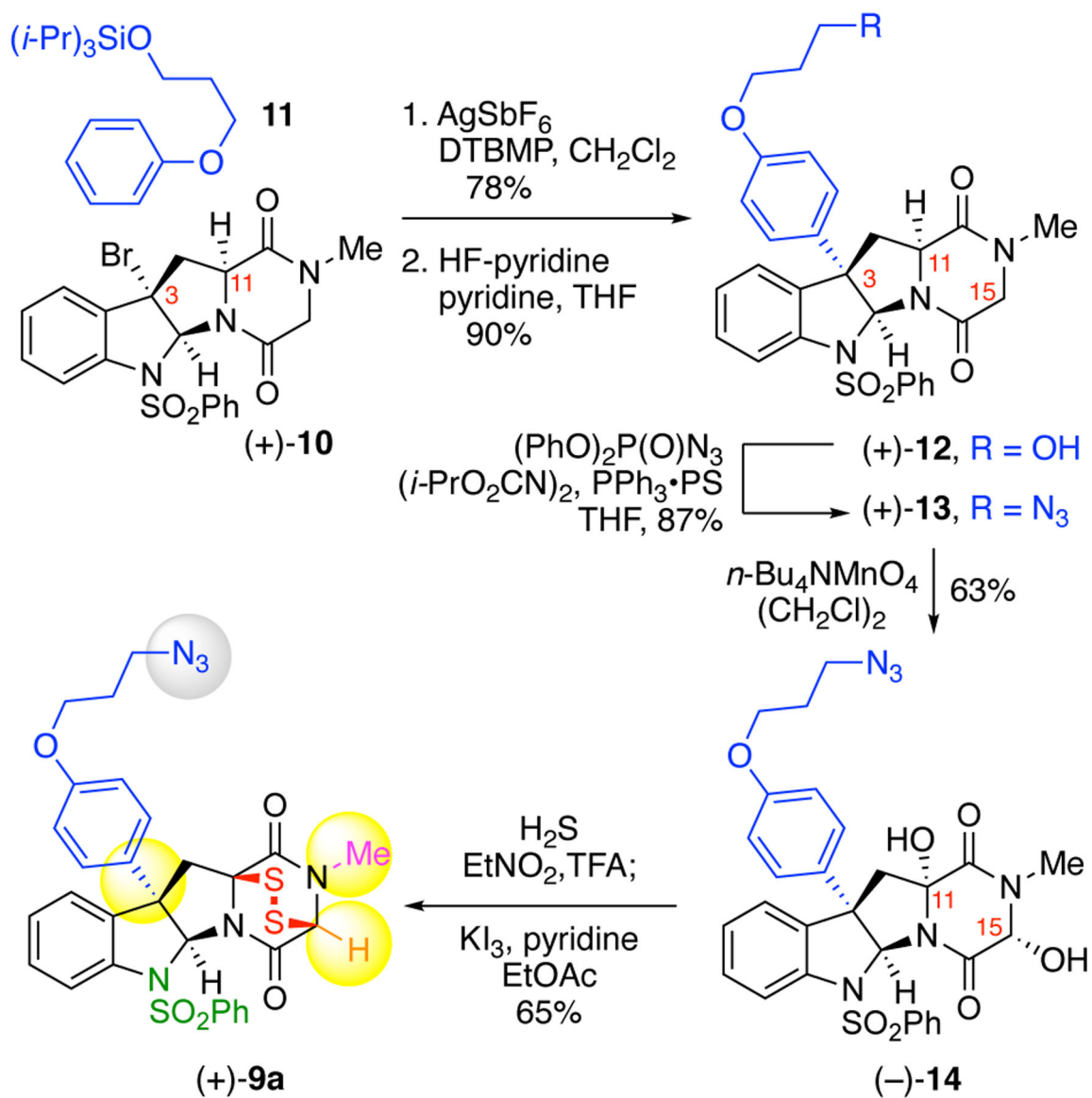
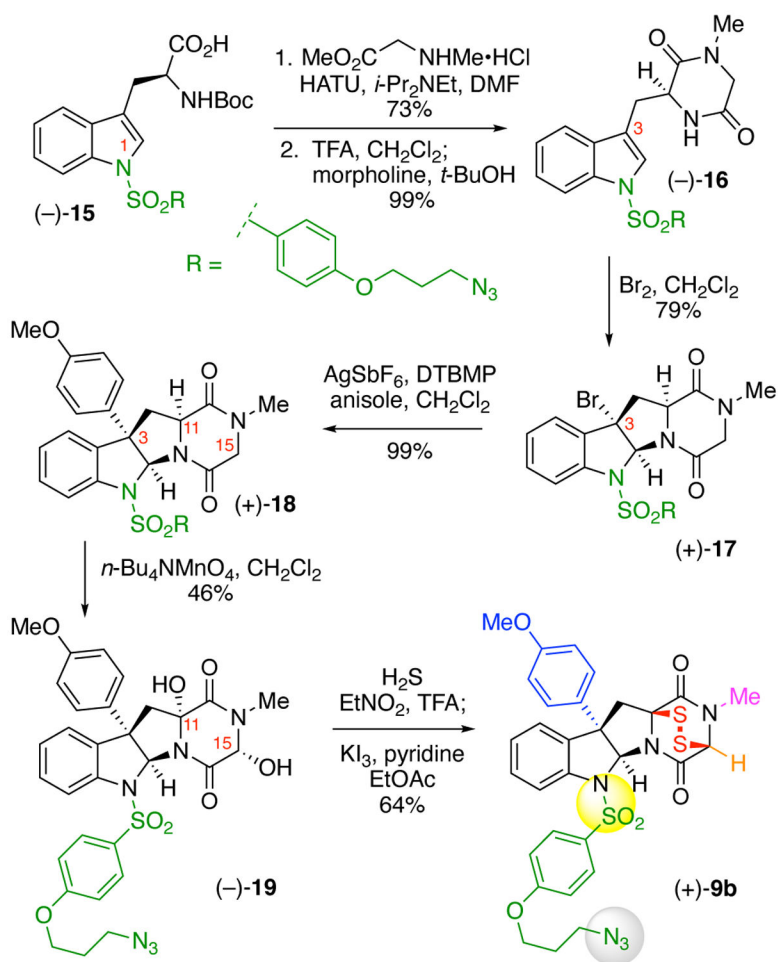**Figure 1.**
Representative natural and unnatural ETPs.
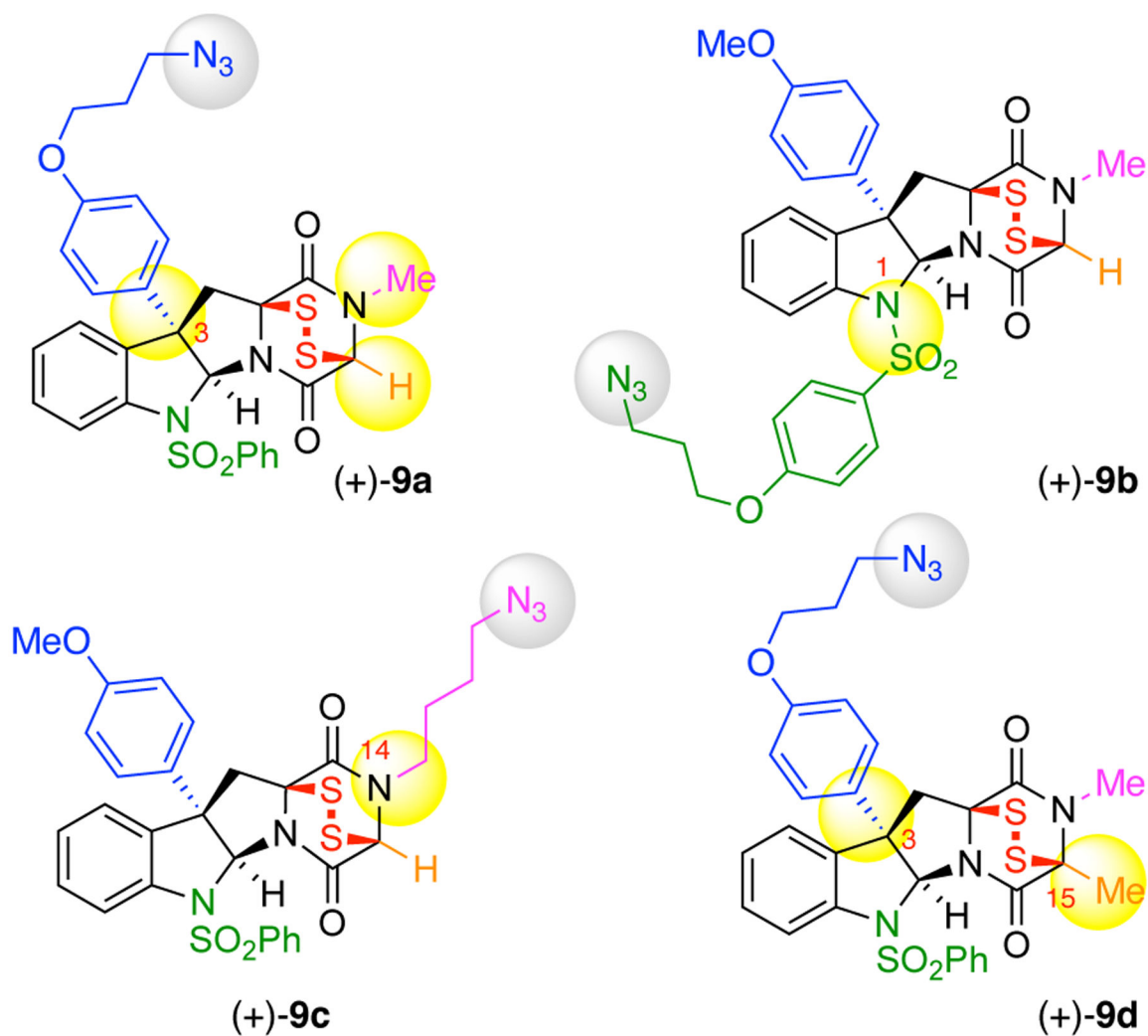
Figure 2.
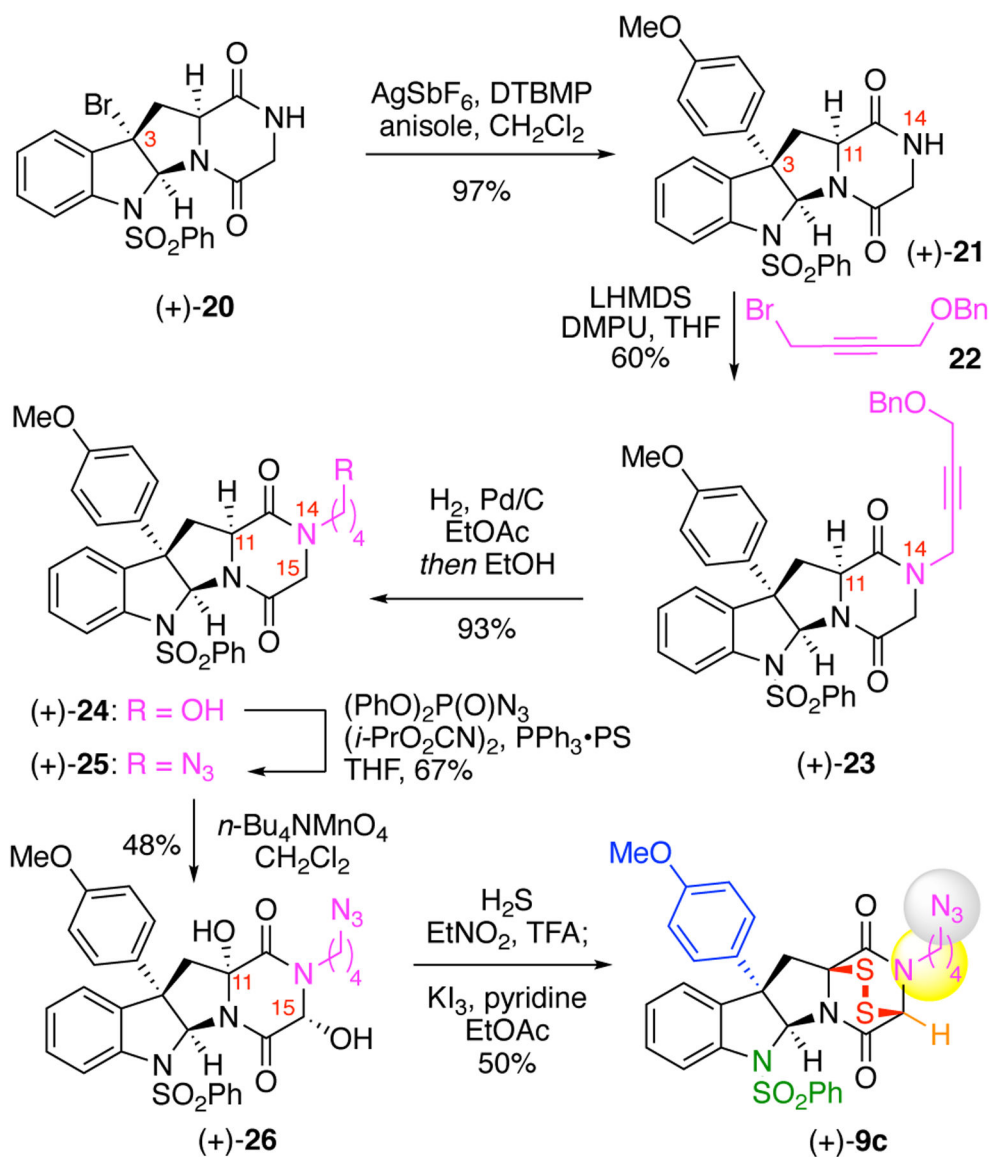Design of structurally diverse complex ETP-azides (+)−**9a**–**d**.
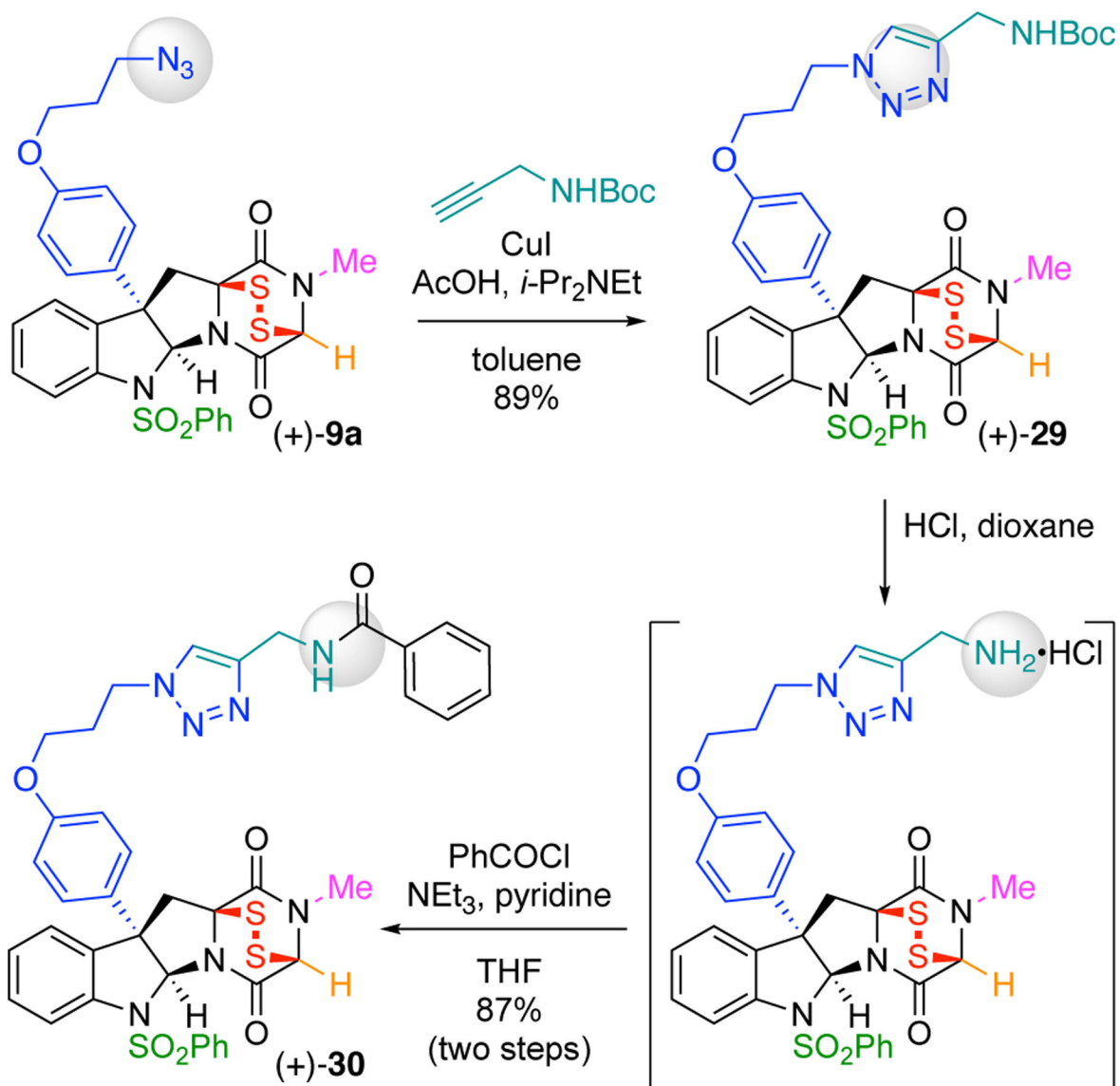
Scheme 1.
Synthesis of designed ETP-azide (+)–**9a**.
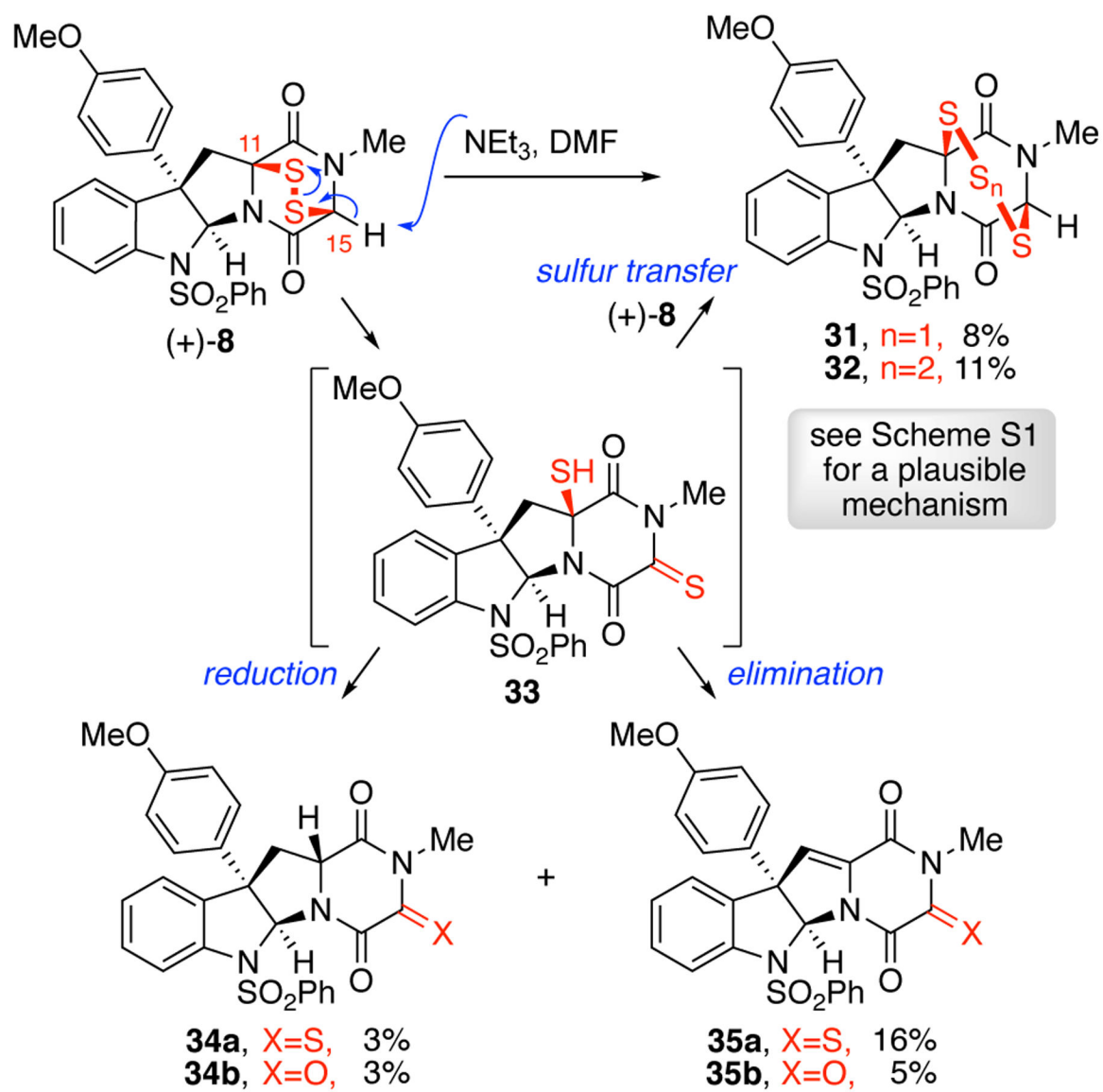
Scheme 2.
Synthesis of designed ETP-azide (+)–**9b**.

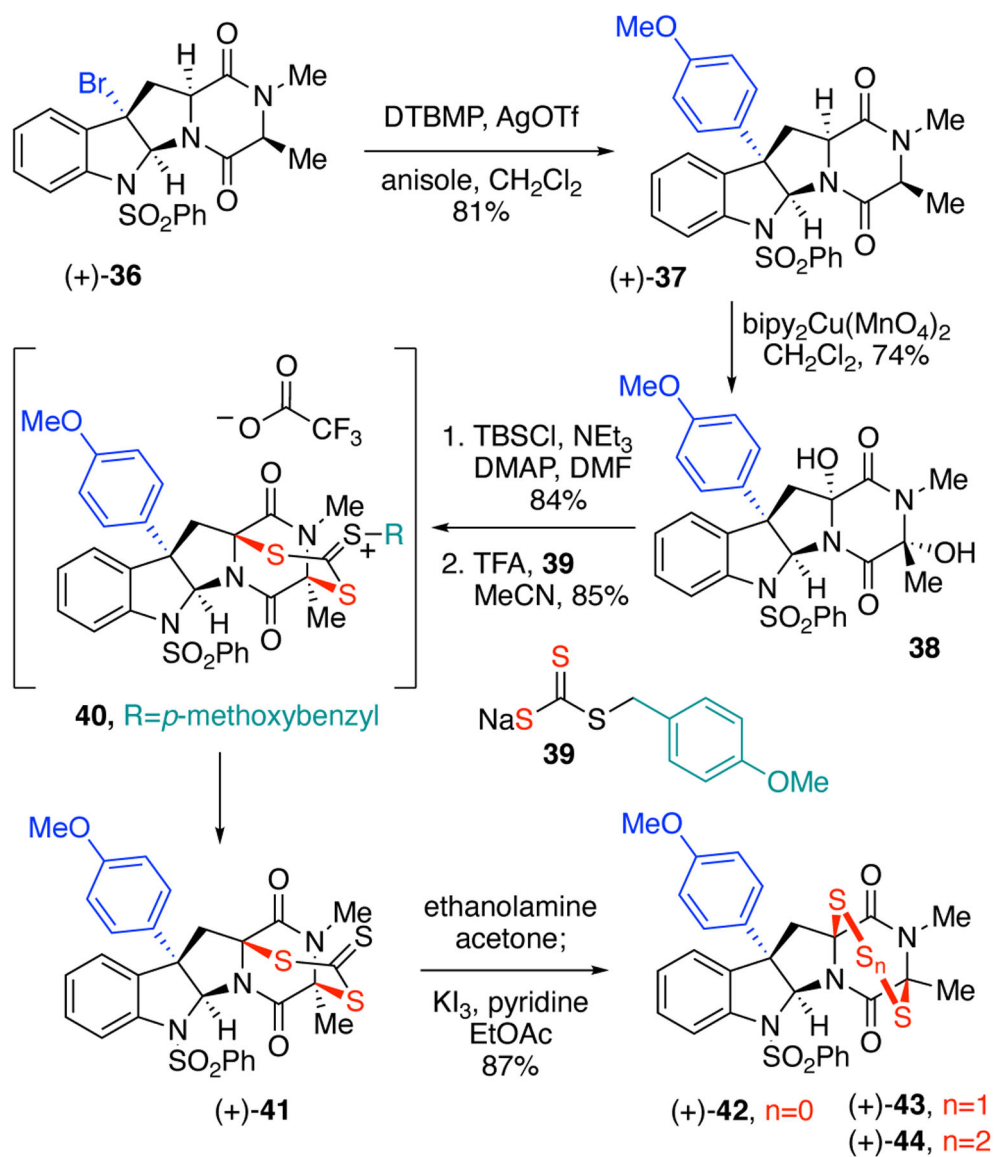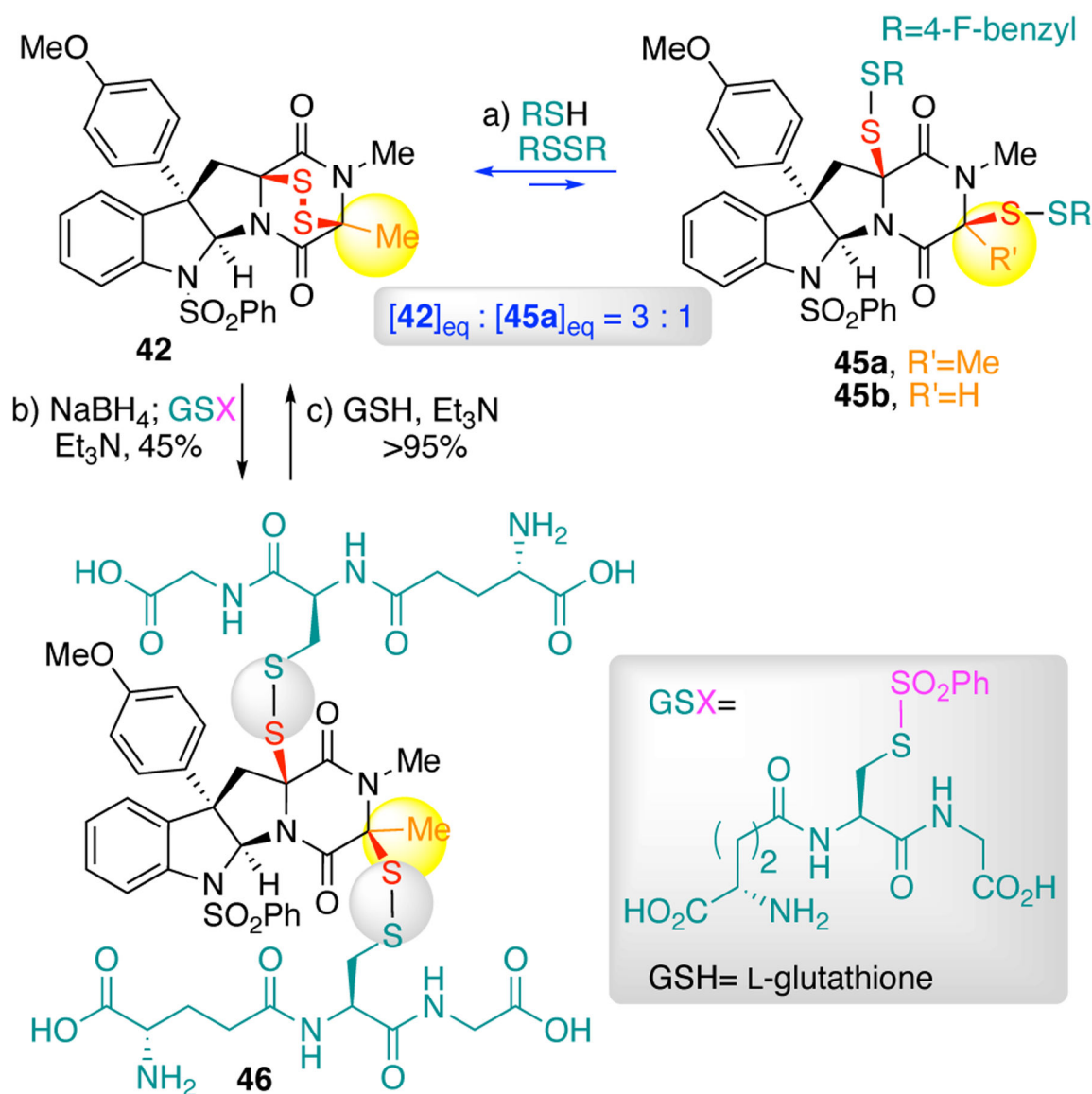**Scheme 3.**
Synthesis of designed ETP-azide (+)–**9c**.

Scheme 4.
Representative derivatization of ETP-azide (+)−**9a**.

Scheme 5.
Base-sensitivity of ETP (+)–**8** and formation of its congeners **31**–**32**.

Scheme 6.
Synthesis of C15-Me ETP (+)−**42**.

Scheme 7.

Thiol-disulfide exchange studies of ETP **42**. Conditions: (a) para-fluorobenzylthiol, (parafluorobenzyl)disulfane, NEt$_3$, THF, 23 °C. (b) NaBH$_4$, MeOH, THF; S-(phenylsulfonyl)-L-glutathione hydrogen chloride, NEt$_3$, MeOH, THF, 23 °C. (c) L-glutathione, NEt$_3$, D$_2$O, CD$_3$CN, 23 °C.
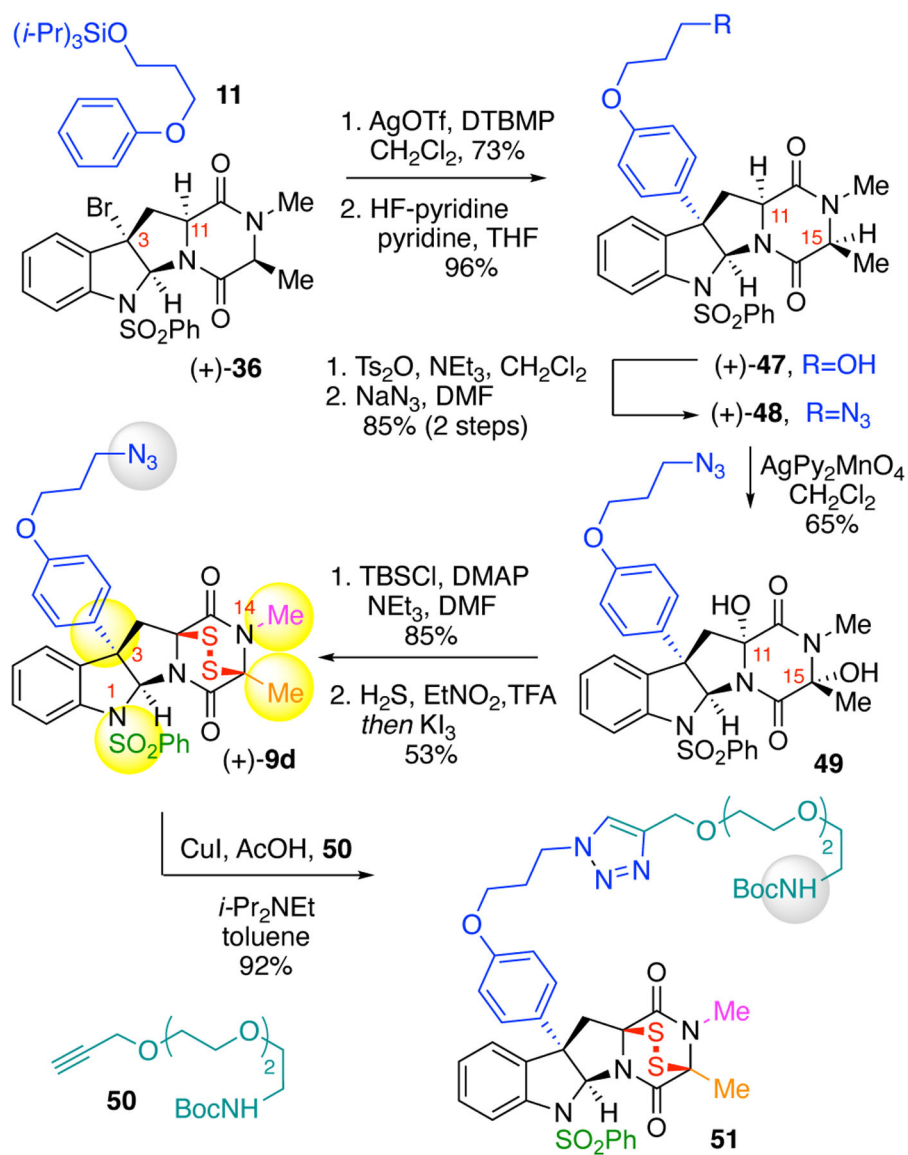
Scheme 8.
Synthesis and Utility of Designed ETP-azide (+)–**9d**.

Table 1.

Derivatization of ETP-azides (+)−**9a**–**c**with alkyne **27**. Conditions:23 ETP-azide (1 equiv), 4-ethynylanisole **27**(5.0 equiv), CuI (0.50–1.5 equiv), acetic acid (1.0–3.0 equiv), *N,N*-diisopropylethylamine (1.0–3.0 equiv), dichloromethane, 23 °C. [a] Toluene used as solvent.

Table 2.

Assessment of Designed ETPs for Cytotoxicity in Five Human Cancer Cell Lines {HeLa (cervical carcinoma), A549 (alveolar adenocarcinoma), MCF7 (breast adenocarcinoma), HCT 116 (colorectal carcinoma), and DU 145 (prostate carcinoma). 72-hour IC_{50} values (in nM) as determined by Cell Titer-Glo (Promega), measuring ATP levels as a surrogate for cell viability. Error is standard deviation of the mean, n 2; IC50 = half maximal inhibitory concentration.

	HeLa	A549	MCF7	HCT 116	DU 145
Alanine-derived dimeric ETP					
(+)-4	0.11 ± 0.14	0.46 ± 0.45	0.30 ± 0.44	0.24 ± 0.29	0.18 ± 0.18
Glycine-derived ETPs					
(+)-8	5.5 ± 1.7	16 ± 9.8	9.2 ± 3.1	6.9 ± 2.9	3.4 ± 4.2
(+)-9a	5.3 ± 0.2	8.8 ± 2.6	7.8 ± 3.6	5.7 ± 0.2	6.9 ± 2.1
(+)-28a	7.9 ± 3.7	25 ± 7.7	7.8 ± 5.9	11 ± 6.3	15 ± 5.6
(+)-29	61 ± 46	753 ± 13	148 ± 58	119 ± 30	80 ± 25
(+)-9b	15 ± 12	76 ± 35	53 ± 48	37 ± 21	44 ± 46
(+)-28b	6.3 ± 5.9	39 ± 12	19 ± 15	20 ± 8.6	16 ± 14
(+)-9c	44 ± 25	143 ± 16	51 ± 7.1	101 ± 7.5	63 ± 22
(+)-28c	14 ± 11	78 ± 15	14 ± 3.3	23 ± 1.9	22 ± 3.5
Glycine-derived bisdisulfide					
45b	4.0 ± 0.1	21 ± 1.1	5.0 ± 2.3	6.9 ± 1.6	5.4 ± 1.9
Alanine-derived ETPs					
(+)-42	32 ± 37	92 ± 87	81 ± 64	374 ± 83	36 ± 43
(+)-9d	136 ± 84	251 ± 307	86 ± 113	348 ± 442	306 ± 385
51	24 ± 29	116 ± 102	82 ± 105	148 ± 148	62 ± 75
Alanine-derived bisdisulfides					
45a	81 ± 26	141 ± 68	90 ± 23	141 ± 20	88 ± 50
46	508 ± 75	910 ± 324	500 ± 152	1096 ± 540	580 ± 216

■ ≤1 nM	■ 1 < x ≤ 25 nM	■ 25 < x ≤ 100 nM	■ 100 < x ≤ 250 nM	■ 250 < x ≤ 1000 nM	■ >1000 nM